Epidermal Growth Factor Receptor Mutations in Small Cell Lung Cancer

Akiko Tatematsu,[1] Junichi Shimizu,[2] Yoshiko Murakami,[4] Yoshitsugu Horio,[2] Shigeo Nakamura,[5] Toyoaki Hida,[2] Tetsuya Mitsudomi,[3] and Yasushi Yatabe[1]

Abstract **Purpose:** The vast majority of epidermal growth factor receptor (*EGFR*) mutations occur in lung adenocarcinoma, and even rare cases of other subtypes with this mutation, such as adenosquamous cell carcinoma, are associated with adenocarcinoma histology. According to this adenocarcinoma-specific nature of *EGFR* mutation, analysis of *EGFR* mutations with small cell lung cancers (SCLC) may provide a clue to its histogenesis.

Experimental Design: The mutational status of the *EGFR* gene was accessed in a cohort of 122 patients with SCLC; all patients were from a single institute. When the *EGFR* mutated, its gene copy number was also examined.

Results: *EGFR* mutations were detected in five SCLCs (4%). The patients were mainly in the light smoker and histologic combined subtype. All but one of the tumors harbored gene amplifications. Notably, in three tumors of the combined SCLC subtype, both components of adenocarcinoma and SCLC harbored an *EGFR* mutation, whereas gene amplification was detected only in the adenocarcinoma component. A partial response was achieved in a patient (with an *EGFR* mutation) who was treated with gefitinib.

Conclusions: Although *EGFR* mutations are rare in SCLC, a combined subtype of SCLC with adenocarcinoma in light smokers may have a chance of harboring *EGFR* mutations. For patients with an *EGFR* mutation, *EGFR* tyrosine kinase inhibitor can be a treatment option. In terms of molecular pathogenesis, it is suggested that some SCLCs may have developed from pre-existing adenocarcinomas with *EGFR* mutations, but the development may not be simply linear, taking into consideration the discordant distribution of *EGFR* amplification.

The vast majority of epidermal growth factor receptor (*EGFR*) gene mutations are detected in lung adenocarcinoma. A comprehensive analysis by Shigematsu and Gazdar reported that non-adenocarcinomatous lung cancers with *EGFR* gene mutations were restricted to <5% of lung cancers (1). Although it is rare in other histologic subtypes, adenosquamous cell carcinoma showed the highest frequency among lung cancers, followed by squamous cell carcinoma and large cell carcinoma. In contrast, small cell carcinoma was not listed among *EGFR*-mutated lung cancers following a comprehensive examination of 1,380 lung tumors, which suggests a different molecular pathogenesis for this type of cancer. However, two patients (who had never smoked), recently reported having *EGFR* mutations with small cell lung cancers (SCLC; refs. 2, 3). In the first case, published in *The New England Journal of Medicine*, the patient with adenocarcinoma was initially treated with erlotinib. The recurrent tumor in the brain consisted of small cell carcinoma, which also harbored an *EGFR* mutation. Because the mutational status of the *EGFR* gene in the initial adenocarcinoma was not addressed, the clonal relationship between the two tumors was not clear. Another case was also a never-smoker who developed widespread SCLC. Mutational analysis revealed a typical *EGFR* gene deletion at exon 19. The tumor responded well to gefitinib treatment, and both primary and metastatic tumors regressed dramatically (3).

The incidence of *EGFR* mutation is quite high among the Japanese (~30-40% of non-small cell lung cancers on average) in contrast to ~10% of patients in the United States and in European countries (1, 4, 5). The clinicopathologic characteristics of patients with *EGFR* mutations include female sex, not smoking, and less frequent p53 mutation (4–6), which are very different from those of SCLC. It is therefore expected that *EGFR* mutations are very rare or absent in SCLC. A comprehensive analysis of *EGFR* mutations in SCLCs has not been reported in the literature; however, we believe it is important to determine its incidence, especially in mutation-endemic countries. In this study, we comprehensively examined a total of 122 SCLCs to address mutation incidence in SCLC.

Authors' Affiliations: Departments of [1]Pathology and Molecular Diagnostics, [2]Thoracic Oncology, [3]Thoracic Surgery, Aichi Cancer Center Hospital, [4]First Department of Pathology, and [5]Department of Pathology, Nagoya University School of Medicine, Nagoya, Japan

Received 2/8/08; revised 5/7/08; accepted 5/10/08.

Grant support: Grant-in-aid (C-19590379) from the Ministry of Education, Culture, Sports, Science, and Technology of Japan.

The costs of publication of this article were defrayed in part by the payment of page charges. This article must therefore be hereby marked *advertisement* in accordance with 18 U.S.C. Section 1734 solely to indicate this fact.

Requests for reprints: Yasushi Yatabe, Departments of Pathology and Molecular Diagnostics, Aichi Cancer Center Hospital, Kanokoden, Chikusa-ku, Nagoya 464-8681, Japan. Phone: 81-52-762-2983; Fax: 81-52-763-5233; E-mail: yyatabezaichi-cc.jp.

doi:10.1158/1078-0432.CCR-08-0332

Translational Relevance

It is well known that epidermal growth factor receptor (*EGFR*) mutations are prevalent in female nonsmokers. However, *EGFR* mutations have recently been reported in some patients with small cell lung cancers (SCLC). In this study, we first examined a large series of SCLCs to address mutation incidence. Because the incidence of *EGFR* mutations differs between the United States and Japan, these data are important in determining the significance of ethnicity and frequency of *EGFR* mutations. As a result, a combined subtype of SCLC with adenocarcinoma in light smokers may have a chance of harboring *EGFR* mutations, although *EGFR* mutations are generally rare in SCLC. Notably, one such patient with an *EGFR* mutation achieved a partial response to gefitinib treatment. Although clinical relevance needs to be examined in more patients, *EGFR* tyrosine kinase inhibitor can be a treatment option for patients with SCLCs harboring an *EGFR* mutation.

Materials and Methods

Patients. Among 150 patients that were diagnosed with SCLC in the last 7 years at the Department of Pathology and Molecular Diagnostics, Aichi Cancer Center in Nagoya, Japan, specimens from 122 patients were available for molecular genetic analysis, and these were the subject for the current study. This series included 102 specimens obtained by biopsy, and 20 from surgically resected tumors. Histologic diagnosis of SCLC was based on the standard criteria defined by WHO classification (7). The study was a part of a comprehensive lung cancer research program, which had been approved by the institutional review board.

EGFR *mutation analysis.* All the specimens were fixed with formalin, and the *EGFR* mutation was analyzed with the method described previously, using an unstained paraffin section (8). This technique allows the detection of tumor cells constituting as little as 5% of a mixture of tumor cells with normal tissue using a single paraffin section. When frozen tissues were available, the mutational status of *EGFR* was accessed with standard reverse transcription-PCR coupled direct sequencing, as described previously (4), in addition to DNA-based analysis. In this assay, the mutational status of the L858R point mutation and the deletion of exon 19 were obtained when we examined paraffin sections, whereas direct sequencing using RNA revealed the mutational status of the whole tyrosine kinase domain.

Copy number analysis of EGFR. Gene amplification was analyzed by fluorescence *in situ* hybridization, using the LSI EGFR SpectrumOrange/CEP 7 SpectrumGreen probe (Vysis; Abbott Laboratories) according to the manufacturer's protocol. Fluorescence *in situ* hybridization was done on serial paraffin sections in the same tissue areas as the gene dosage analysis. A more than 4-fold increase of *EGFR* gene signals relative to CEP7 signals was considered a gene amplification. The results were confirmed by TaqMan-based gene dosage analysis as described previously (9).

Statistical analysis. Fisher's exact test for independence and unpaired *t* tests were used to show the correlation of clinicopathologic variables with EGFR mutation. $P < 0.05$ was considered statistically significant.

Results

SCLCs with EGFR *mutation.* Among 122 SCLCs examined (Table 1), we found *EGFR* mutations in five cases (4%). The mutations included L858R point mutations (three patients), a G719A point mutation (one patient), and a 15-bp deletion in exon 19 (one patient). Both frozen and paraffin tissues of 10 tumors, 2 of which harbored the above *EGFR* mutation, were available for analysis. They were examined using both reverse transcription-PCR coupled sequencing and assays for paraffin sections. The results were identical to those of the other analysis.

Clinicopathologic features of SCLCs with EGFR *mutations.* *EGFR* mutations were restricted to a very minor proportion (5 of 122; 4%) of SCLCS, and the clinicopathologic features of the patients with the mutation showed a trend similar to those of patients without the mutation. There were no significant differences in age, sex, and clinical stage at presentation. In contrast, accumulated smoking dose (pack-years) in patients with the mutation was much lower, and the difference was statistically significant (unpaired *t* test, $P = 0.02$). Indeed, three of the five patients with *EGFR* mutations were smokers with less than 40 pack-years. It is of note that one of the five patients was treated with gefitinib, and partial response was observed (case 2).

Morphologic features of SCLC with EGFR *mutations.* There are two subtypes of SCLC in the current WHO classification; thus, we examined whether the morphologic subtypes were associated with *EGFR* mutations. The combined subtype constituted a minor proportion (15 of 122, 12%) in this series, and three of them were positive for *EGFR* mutations (Table 1). Preferential mutation in the combined type were statistically significant (Fisher's exact test, $P < 0.01$). In two cases of the combined subtype (cases 1 and 3), SCLC components consisted of only a part of the nodule, and adenocarcinoma components constituted the predominant part. The representative morphologic features are displayed in Fig. 1. The other combined subtype (case 5) showed a mixture of SCLC and adenocarcinoma components throughout the tumor.

EGFR *amplification in SCLCs.* We have recently reported that *EGFR* amplification occurs in association with *EGFR* mutation (9). We therefore examined the EGFR gene copy number in the five SCLCs with *EGFR* mutations. Four of them showed gene amplification (Table 2), and the signals of the EGFR gene were loosely clustered (Fig. 2), suggesting a high degree of amplification, as is the case in homogeneously staining region patterns. Notably, three cases of combined SCLC subtypes harbored *EGFR* amplifications only in the adenocarcinoma component, but not in the SCLC component (Fig. 2).

Discussion

SCLC is a distinct neoplasm in terms of clinical aggressiveness, despite its high response to both chemotherapy and irradiation therapy. This aggressive cancer does not confer to

Table 1. Clinicopathologic features of SCLCs with and without *EGFR* mutations

	Mutated	Wild-type	*P*
No. of patients (total, $N = 122$)	5	117	
Age (median)	69	67	n.s.
Sex (female/male)	2/3	14/103	n.s.
Smoking history (median pack-years)	30	54	0.020
Disease stage (limited/extended disease)	4/1	81/33	n.s.
Histologic type (conventional/combined)	2/3	105/12	0.013

Abbreviation: n.s., not significant.

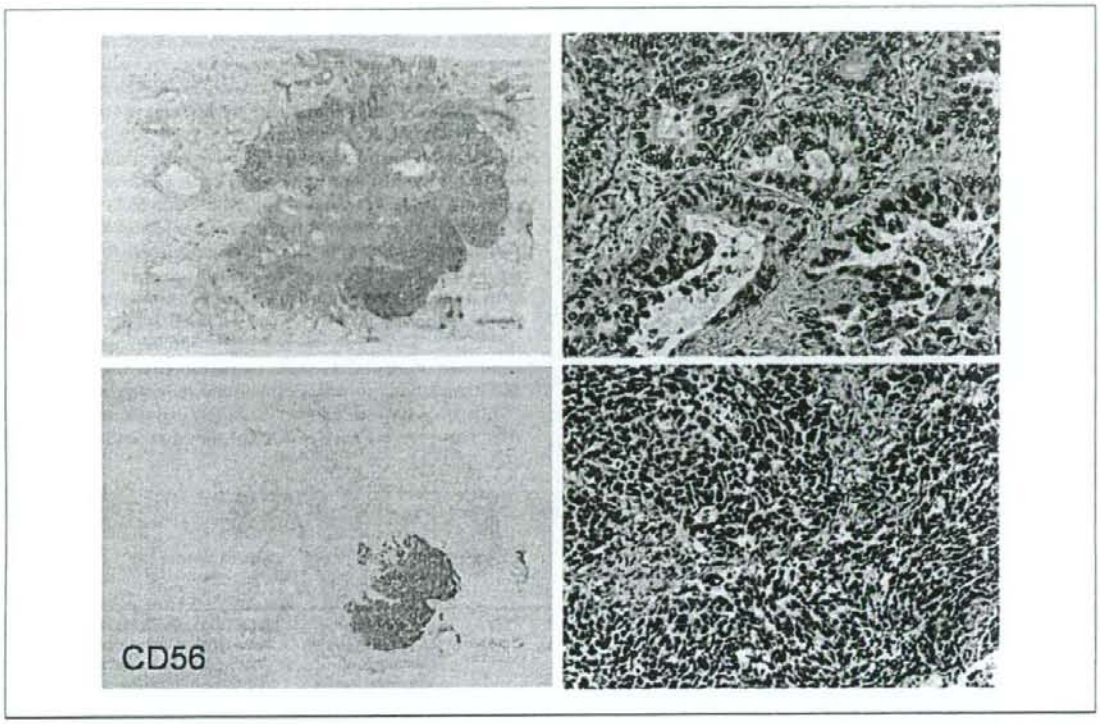

Fig. 1. Representative morphology of combined small cell carcinoma and adenocarcinoma (case 3). Approximately two-thirds of the area of the nodule (*top left*) consisted of an adenocarcinoma component, whereas the other area showed SCLC. Discrete expression of CD56 (neural cell adhesion molecule) corresponds to the component of SCLC (*bottom left*). High-power views of each component of adenocarcinoma (*top right*) and SCLC (*bottom left*). Both components harbor identical L858R *EGFR* mutations, although *EGFR* gene amplification was restricted to the adenocarcinoma component.

the lung, and it can develop in organs other than the lung, all of which share distinctive pathologic and immunohistochemical features, irrespective of their site of origin. These extrapulmonary carcinomas are characterized by frequent admixture with conventional carcinoma of the originating organ, such as adenocarcinoma in gastrointestinal tumors, and squamous cell carcinoma in head and neck cancers. This is true in SCLC. Nicholson et al. reported that 28 of 100 surgically resected SCLCs had a histologic component of non–small cell lung cancers (10). In our study, *EGFR* gene mutation was detected in 5 of 122 SCLCs. Because *EGFR* mutation was quite specific for adenocarcinoma, it is suggested that SCLCs with *EGFR* mutations are associated with adenocarcinoma. Indeed, three of the five combined SCLC had an adenocarcinoma component but not a squamous cell carcinoma component.

It has been suggested that the amine-precursor uptake and decarboxylase cells described by Pearse in 1969 (11) are the putative original cells of small carcinoma. These cells were described as comprising a neuroendocrine system in many organs, and as having ultrastructural features shared by small cell carcinomas. However, this hypothesis cannot explain the existence of combined SCLC, which is an admixture of small cell carcinoma and conventional adenocarcinoma or squamous cell carcinoma. Therefore, a multipotential cancer stem cell capable of divergent differentiation has been suggested as a putative origin of small cell carcinoma. Alternatively, the SCLC component may arise as a consequence of undifferentiated transformation from conventional carcinoma. Case 2 in the present study supported the latter scenario, because SCLC is the only component that metastasized to the lymph nodes. Furthermore, the vast majority of lung cancers harboring *EGFR* mutations are adenocarcinomas, supporting the idea that the adenocarcinomas existed prior to the development of SCLC in at least three of the cases of SCLC with *EGFR* mutations.

However, the results of *EGFR* amplification analyses support the former possibility. In three cases of combined subtype of SCLC with an *EGFR* mutation, only the adenocarcinoma component, not the SCLC component, harbored the amplification. This is in contrast to the uniform detection of *EGFR* mutations in both components. Because *EGFR* mutations in SCLC are rather rare, it is unlikely that the two components are independent of their origin. Rather, it is believed that they originated from a common ancestor. Therefore, it is suggested that the mutation occurred before a point branching off to SCLC and adenocarcinoma components, whereas gene amplification was acquired after that point. Cases 3 and 5 may be considered to have followed this scenario. However, case 1 was inconsistent with it because SCLC emerged after the therapy.

In case 1, the initial adenocarcinoma harbored both *EGFR* mutation and amplification. Subsequently, SCLC, which lacked

gene amplification, developed after the chemotherapy and gefitinib therapy. It was unlikely that the amplification was removed from cancer cells due to therapy. We have recently reported heterogeneous distribution of *EGFR* amplification in lung adenocarcinoma (9), and thus we suggested that only a clone without amplification was selected, survived, and was subsequently transformed to SCLC. The reported SCLC with *EGFR* mutation followed this pattern of progression (2, 3, 12), and lack of *EGFR* expression in SCLC may be a clue to this phenomenon. Under heavy selection pressure by gefitinib therapy, only a clone which is independent of *EGFR*-driven growth signals has a chance to expand. Transformation to SCLC fulfills this condition because *EGFR* expression in the SCLC was at a very low or undetectable level (13–15). Indeed, the SCLC component lacked *EGFR* expression, in contrast to positive expression in the initial adenocarcinoma and adenocarcinoma components (data not shown). This may be another mechanism for tolerance to the *EGFR* tyrosine kinase inhibitor, in addition to secondary genetic alterations.

Clinically, it is noteworthy that a partial response was achieved in one of the patients with an *EGFR* mutation who was treated with gefitinib. Because *EGFR* expression is at a very low or undetectable level in SCLC, it would be expected that *EGFR* tyrosine kinase inhibitors are not effective against SCLC even if the *EGFR* is mutated. However, a similar marked reduction of such cancers by *EGFR* tyrosine kinase inhibitor treatment has also been reported (2, 3). *EGFR* tyrosine kinase inhibitors may be a treatment option for SCLC with *EGFR* mutations, and a mutation test may be helpful to select such patients in addition to clinical characteristics, including the light smoker and histologic combined subtypes.

In summary, we examined 122 SCLCs and found 5 (4%) of them harboring *EGFR* mutations. The SCLCs with *EGFR* mutations were seen in the light smoker and histologic combined subtypes. Because of the specific involvement of *EGFR* mutations in adenocarcinoma, it is suggested that the SCLCs may have developed from pre-existing adenocarcinomas. However, we have concluded that this development may

Table 2. Clinicopathologic features of five SCLCs with *EGFR* mutations

Case	Sex/Age (y)	Pack-years smoking	*EGFR* mutation	*EGFR* amplification	Stage	Sample and histologic subtype	Clinical course
1	F/36	0	L858R	Amplified (>6)*	ED	Resected tumor; combined type (diagnosis of adenocarcinoma with a biopsy prior to surgery)	Stage IV adenocarcinoma was treated with CBDCA and PAC, followed by gefitinib, because of positive EGFR mutation with a biopsy specimen. Partial response was achieved but the tumor regrew. It was surgically resected, and histologically revealed to be combined small and adenocarcinoma
2	M/81	40	G719A	Amplified (>6)	ED	Biopsy specimen; conventional type	Stage IV SCLC was treated with gefitinib, because of the detection of G719A mutation using a lung biopsy specimen. A partial response was obtained
3	M/69	30	L858R	Amplified (>6)*	LD	Biopsy specimen, combined type	A lung cancer ($cT_1N_0M_0$) was surgically removed, and subsequent pathologic examination revealed combined SCLC. Adjuvant chemotherapy (CDDP and CPT-11) were administered. The patient is alive without recurrence
4	F/89	2.5	L858R	Low polysomy	LD	Biopsy specimen; conventional type	A biopsy specimen for lung cancer ($cT_2N_0M_0$) was diagnosed as SCLC. The patient refused any therapy, and was not a part of follow-up
5	M/65	67.5	Ex.19Del	Amplified (>6)*	LD	Resected tumor; combined type (cytological diagnosis of SCLC prior to surgery)	$cT_1N_1M_0$ cancer was treated with CDDP and TXT, followed by surgical resection of the tumor. Combined SCLC was revealed, and the patient was treated with adjuvant chemotherapy and irradiation. Three years later, SCLC recurred

Abbreviations: F, female; M, male; LD, limited disease; ED, extended disease; CBDCA, carboplatin; PAC, paclitaxel; CDDP, cisplatin; CPT-11, irinotecan.
* Only in the adenocarcinoma component.

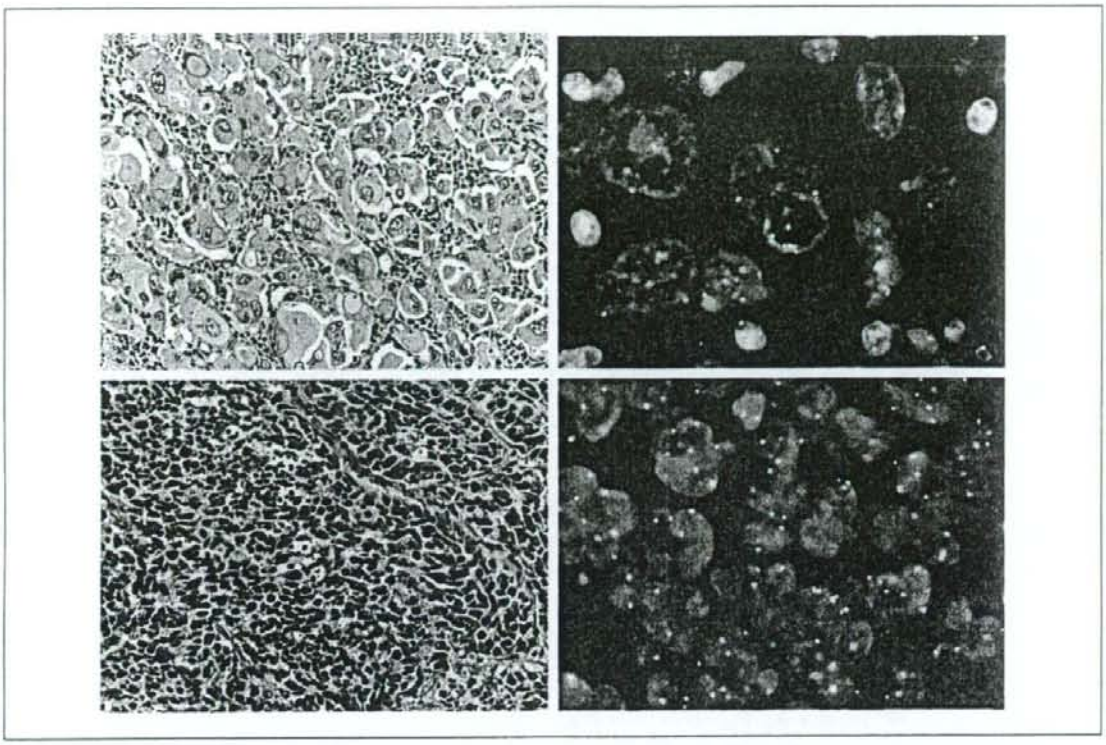

Fig. 2. *EGFR* amplification in SCLC with *EGFR* mutation (case 1). A female nonsmoker who had developed stage IV adenocarcinoma was treated with carboplatin and paclitaxel. The tumor recurred at the neck lymph node (*top left*), which was biopsied. Because molecular analysis using the tissue revealed a L858R mutation, she was subsequently treated with gefitinib. Although the tumor responded initially, rapid regrowth of the lung nodule was evident, and it was removed surgically. The SCLC component constituted most of the regrown nodule. *EGFR* mutation was detected in both adenocarcinomas in the lymph node and in the regrown SCLC, *EGFR* amplification was identified only in the adenocarcinoma but not in the regrown SCLC (*right*).

not be simply linear, considering the discordant distribution of EGFR amplification.

Disclosure of Potential Conflicts of Interest

T. Mitsudomi has a minor conflict with AstraZeneca, Chugai Pharm, Astellas, Daiichi-Sankyo, Sanofi-Aventis, Taiho Pharm, and Bristol Meyers.

Acknowledgments

The authors thank Noriko Shibata for her excellent technical assistance with the molecular genetic experiments, Edwin L. Carty for English editing, and Hiroji Ishida and the members of the Department of Pathology, Aichi Cancer Center, for their assistance with the preparation of paraffin sections.

References

1. Shigematsu H, Gazdar AF. Somatic mutations of epidermal growth factor receptor signaling pathway in lung cancers. Int J Cancer 2006;118:257–62.
2. Zakowski MF, Ladanyi M, Kris MG. EGFR mutations in small-cell lung cancers in patients who have never smoked. N Engl J Med 2006;355:213–5.
3. Okamoto I, Araki J, Suto R, Shimada M, Nakagawa K, Fukuoka M. EGFR mutation in gefitinib-responsive small-cell lung cancer. Ann Oncol 2006;17:1028–9.
4. Kosaka T, Yatabe Y, Endoh H, Kuwano H, Takahashi T, Mitsudomi T. Mutations of the epidermal growth factor receptor gene in lung cancer: biological and clinical implications. Cancer Res 2004;64:8919–23.
5. Shigematsu H, Lin L, Takahashi T, et al. Clinical and biological features associated with epidermal growth factor receptor gene mutations in lung cancers. J Natl Cancer Inst 2005;97:339–46.
6. Marchetti A, Martella C, Felicioni L, et al. EGFR mutations in non-small-cell lung cancer: analysis of a large series of cases and development of a rapid and sensitive method for diagnostic screening with potential implications on pharmacologic treatment. J Clin Oncol 2005;23:857–65.
7. Travis WD, Brambilla E, Mueller-Hermelink HK, Harris CC, editors. Pathology and genetics of tumours of the lung, pleura, thymus and heart. Lyon: IARC Press; 2004.
8. Yatabe Y, Hida T, Horio Y, Kosaka T, Takahashi T, Mitsudomi T. A rapid, sensitive assay to detect EGFR mutation in small biopsy specimens from lung cancer. J Mol Diagn 2006;8:335–41.
9. Yatabe Y, Takahashi T, Mitsudomi T. Epidermal growth factor receptor gene amplification is acquired in association with tumor progression of EGFR-mutated lung cancer. Cancer Res 2008;68:2106–11.
10. Nicholson SA, Beasley MB, Brambilla E, et al. Small cell lung carcinoma (SCLC): a clinicopathologic study of 100 cases with surgical specimens. Am J Surg Pathol 2002;26:1184–97.
11. Pearse AG. The cytochemistry and ultrastructure of polypeptide hormone-producing cells of the APUD series and the embryologic, physiologic and pathologic implications of the concept. J Histochem Cytochem 1969;17:303–13.
12. Morinaga R, Okamoto I, Furuta K, et al. Sequential occurrence of non-small cell and small cell lung cancer with the same EGFR mutation. Lung Cancer 2007;58:411–3.
13. Cerny T, Barnes DM, Hasleton P, et al. Expression of epidermal growth factor receptor (EGF-R) in human lung tumours. Br J Cancer 1986;54:265–9.
14. Kaseda S, Ueda M, Ozawa S, Ishihara T, Abe O, Shimizu N. Expression of epidermal growth factor receptors in four histologic cell types of lung cancer. J Surg Oncol 1989;42:16–20.
15. Sobol RE, Astarita RW, Hofeditz C, et al. Epidermal growth factor receptor expression in human lung carcinomas defined by a monoclonal antibody. J Natl Cancer Inst 1987;79:403–7.

Phase I/II Pharmacokinetic and Pharmacogenomic Study of *UGT1A1* Polymorphism in Elderly Patients With Advanced Non–Small Cell Lung Cancer Treated With Irinotecan

N Yamamoto[1], T Takahashi[1], H Kunikane[2], N Masuda[3], K Eguchi[4], M Shibuya[5], Y Takeda[6], H Isobe[7], T Ogura[8], A Yokoyama[9] and K Watanabe[2]

This phase II study investigated the recommended dose (RD) of irinotecan (CPT-11) by dose escalation in elderly (≥70 years) chemotherapy-naive Japanese patients with advanced non–small cell lung cancer. *UGT1A1*28* and **6* polymorphisms and pharmacokinetics were also investigated. Thirty-seven patients received the RD, 100 mg/m^2 of intravenous CPT-11, on days 1 and 8 of each 3-week cycle in phase II. The overall response rate was 8.1%. The median survival time was 441 days, and time to progression was 132 days. A significant correlation was observed between the incidence of grade 3/4 neutropenia and area under the time-concentration curve (AUC) values of SN-38. A reduction in AUC ratios ($AUC_{SN\text{-}38G}/AUC_{SN\text{-}38}$) and a rise in incidence of grade 3/4 neutropenia were observed with increase in polymorphism. The regimen was well tolerated and provided good disease control and promising survival effects. An analysis of the influence of *UGT1A1*28* and **6* polymorphisms provides useful information for the prediction of CPT-11-related hematological toxicity.

Lung cancer is the most common fatal cancer in Japan and in Western countries.[1] The majority of cases of advanced non–small cell lung cancer (NSCLC) are found among patients aged >65 years, and the number of such cases is predicted to rise with increases in the numbers of the elderly.[2,3]

Chemotherapy has been shown to yield better results than best supportive care in NSCLC patients in terms of survival and quality of life.[4] Platinum-based regimens containing a third-generation agent, including irinotecan (CPT-11), taxanes, gemcitabine (GEM), and vinorelbine (VNR), have been the mainstream treatment for patients with NSCLC.[5] However, these regimens have been associated with high toxicity while providing no survival benefit in elderly patients. Several prospective randomized trials have investigated optimal chemotherapy in patients aged ≥70 years with advanced NSCLC.[6–9] The regimens investigated have included VNR monotherapy,[6] GEM plus VNR vs. VNR alone,[7] VNR vs. GEM vs. VNR plus GEM,[8] and docetaxel (DOC) vs. VNR.[9] The results of the Elderly Lung Cancer Vinorelbine Italian Study (ELVIS) led to the recommendation that VNR monotherapy be used as first-line therapy in elderly patients with advanced NSCLC.[6] On the basis of these studies, and given that GEM is less active than VNR, many researchers now recommend VNR monotherapy.

CPT-11 is a semi-synthetic camptothecin derivative with topoisomerase I–inhibiting activity.[10–12] CPT-11, a prodrug, is converted to its active metabolite, SN-38 (7-ethyl-10-hydroxycamptothecin), by carboxylesterase, which is 100- to 1,000-fold more cytotoxic than CPT-11. Further hepatic metabolism by uridine diphospho-glucuronosyl-transferases (UGTs) converts SN-38 to its inactive metabolite, SN-38 glucuronide (SN-38G).[10–12]

Phase III clinical studies on CPT-11 conducted in NSCLC patients have included a comparison we made of CPT-11

[1]Thoracic Oncology Division, Shizuoka Cancer Center, Sunto-gun, Japan; [2]Department of Respirology, Yokohama Municipal Citizen's Hospital, Yokohama, Japan; [3]Department of Respiratory Medicine, Kitasato University School of Medicine, Sagamihara, Japan; [4]Department of Respirology, Tokai University School of Medicine, Isehara, Japan; [5]Department of Internal Medicine, Tokyo Metropolitan Komagome Hospital, Tokyo, Japan; [6]Department of Respiratory Medicine, International Medical Center of Japan, Tokyo, Japan; [7]Department of Medical Oncology, KKR Sapporo Medical Center, Sapporo, Japan; [8]Department of Respiratory Medicine, Kanagawa Cardiovascular and Respiratory Center, Yokohama, Japan; [9]Department of Internal Medicine, Niigata Cancer Center Hospital, Niigata, Japan. Correspondence: N Yamamoto (n.yamamoto@scchr.jp)

Received 7 February 2008; accepted 13 June 2008; advance online publication 6 August 2008. doi:10.1038/clpt.2008.152

monotherapy, a cisplatin-plus-vindesine group (VDS-P), and a cisplatin-plus-CPT-11 (IP) group.[13] The response rate in the CPT-11 monotherapy group in a subset of elderly patients (aged 70–75 years) in that study was 40.0%, similar to that in the VDS-P group (43.5%). Moreover, the response rate was higher in the IP group (60.9%) than in those undergoing either of the other two regimens. Interestingly, survival time was better in the CPT-11 monotherapy group (44.3 weeks) than in the VDS-P group (35.7 weeks). As for adverse events in this subset of elderly patients, although the incidence of diarrhea tended to be higher in the CPT-11 monotherapy group, leukopenia, neutropenia, nausea/vomiting, and anorexia were all mild. Because these findings suggested that CPT-11 monotherapy might be a useful regimen in elderly patients with NSCLC, the regimen was investigated in this prospective study.

Severe CPT-11-associated diarrhea and myelosuppression have been reported as dose-limiting toxicities (DLTs).[14,15] These effects correlate significantly with the area under the time-concentration curve (AUC) values of CPT-11 and its active metabolite SN-38 and glucuronized SN-38.[14,15] Among UGT isoforms, *UGT1A1* is believed to be responsible for SN-38 glucuronidation and is also thought to be involved in the large inter-individual variations seen in SN-38 pharmacokinetics.[16] Several studies have reported a correlation between the adverse effects of CPT-11 and the presence of *UGT1A1* polymorphisms including *UGT1A1*28* and *UGT1A1*6*.[17–19] Ethnic differences have also been reported in the distribution of these polymorphisms, with higher incidences of *UGT1A1*6* occurring in Asians (including Japanese) than in Caucasians.[20–22] This suggests that *UGT1A1* polymorphism is an important determining factor in the efficacy and toxicity of CPT-11 and that pharmacogenetics-guided dosing of CPT-11 may help to individualize the dose of CPT-11 and moderate its toxicity in cancer patients.

We performed phase I and II studies involving CPT-11 monotherapy on days 1 and 8 of a 3-week cycle in elderly patients with NSCLC to determine the DLT, maximum-tolerated dose (MTD), and recommended dose (RD) and to investigate the antitumor effect and safety of the RD. Further, a prospective analysis of *UGT1A1* mutations was performed, and we investigated the relationship between the presence of these polymorphisms and the occurrence of adverse events. We also analyzed the variation in the pharmacokinetics of CPT-11 and its metabolites in elderly patients.

RESULTS

Patient characteristics

Between April 2003 and March 2006, 46 patients with stage IIIB/IV NSCLC were enrolled. In the overall study population, 76% of the patients (35 of 46) had stage IV disease, and 69.5% (32 of 46) had adenocarcinoma. Twelve patients were enrolled and treated in phase I. Six patients were treated at dose level 1 (60 mg/m^2), three patients at dose level 2 (80 mg/m^2), and three patients at dose level 3 (100 mg/m^2). DLT of persistent grade 2 leukopenia was observed in one patient at dose level 1, and an additional three patients were enrolled at this dose level. No further DLTs were observed in these patients or in patients receiving 80 or 100 mg/m^2. Therefore the MTD was not reached in this study, and the RD was set at 100 mg/m^2, in accordance with the study protocol described in "Methods."

In phase II, 34 additional patients were treated at 100 mg/m^2, making a total of 37 patients treated with the RD. **Table 1** shows the selected baseline demographics and disease characteristics of the patients treated with the RD. There were 25 men and 12 women, with a median age of 76 years (range: 71–88).

The median number of treatment cycles in phase II was 4.0 (range: 1–18); 37.8% of patients (14 of 37) received five or more cycles, and the percentage of patients with 6-month or longer treatment was ~22%. The relative dose intensity was 90.0%. Twenty-five of the 37 patients went on to second-line therapy comprising gefitinib (in 7 patients, 28%), different regimens of CPT-11 (7 patients, 28%), carboplatin/paclitaxel (4 patients, 16%), DOC (3 patients, 12%), GEM (3 patients, 12%), and S-1/cisplatin (1 patient, 4%).

Response and survival

All 37 patients (including 3 patients in phase I) who received the RD were evaluated to determine the overall response rate. The overall response rate was 8.1% (complete response (CR): 0, partial response (PR): 3; 3/37, 95% confidence interval: 1.7–21.9), and the disease control rate was 21.6% (8/37, 95% confidence interval: 9.8–38.2). The median survival time (MST) was 441 days after a median follow-up of 440 days, and the 1-year survival rate was 56.8% (**Figure 1**). The median time to progression (TTP) was 132 days.

Toxicity

In phase I, persistent grade 2 leukopenia was observed in one patient who received treatment at level 1, and the second cycle could not be started until day 30. This adverse event was therefore regarded as a DLT. Adverse events that occurred in phase II are summarized in **Table 2**. The most frequently observed hematological toxicity (grade 3/4) was neutropenia (27.0%).

Table 1 Demographics of patients treated with irinotecan 100 mg/m^2

Characteristic	No. of patients (N = 37)	%
Sex		
Male	25	68
Female	12	32
Age (years)		
Median	76.0	
Range	71–88	
Performance status		
0	11	30
1	26	70
Histology		
Adenocarcinoma	25	68
Other	12	32
Stage		
IIIB	10	27
IV	27	73

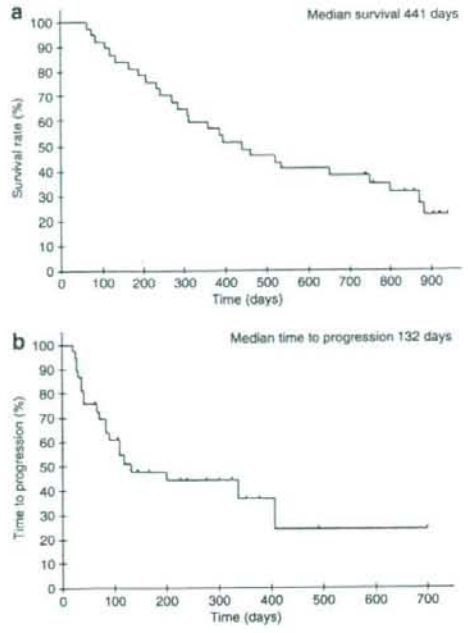

Figure 1 Elderly patients with advanced NSCLC treated with irinotecan. (**a**) Kaplan–Meier overall survival curve and (**b**) time-to-progression curve.

Table 2 Summary of adverse events in phase II (all courses)

	CPT-11 dose: 100 mg/m² (*N* = 37)	
Adverse event, patients	Any event	Grade 3/4 (%)
Leukopenia	26	9 (24.3)
Neutropenia	28	10 (27)
Anemia	27	4 (10.8)
Thrombocytopenia	1	1 (2.7)
Febrile neutropenia	0	0 (0)
Diarrhea	28	3 (8.1)
Nausea	23	4 (10.8)
Vomiting	13	0 (0)
Anorexia	31	9 (24.3)
Fatigue	14	1 (2.7)

Adverse events were assessed using National Cancer Institute Common Toxicity Criteria.

Frequently observed nonhematological toxicities (grade 3/4) included nausea (10.8%), anorexia (24.3%), and diarrhea (8.1%). Grade 4 toxicity (neutropenia) occurred in one patient who received treatment at level 3. Treatment-related death occurred in one patient, due to interstitial pneumonia.

Relationship of *UGT1A1**6 and *28 polymorphisms to pharmacokinetics and toxicity of CPT-11

The analysis of *UGT1A1* genotypes was performed in the 36 patients who had provided informed consent, and their

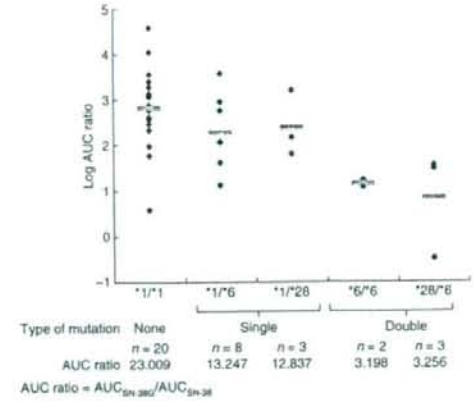

Figure 2 Comparison of area under the time-concentration curve (AUC) ratios by type of polymorphism in 36 patients treated with 100 mg/m² of irinotecan. The pharmacokinetic profile of irinotecan was affected to similar extents by **28* heterozygous and **6* heterozygous mutations, and by **6* homozygous and **6/*28* heterozygous mutations. The lines indicate geometric mean and the *y*-axis represents the log scale.

Table 3 Relationships between polymorphisms and adverse events and pharmacokinetic profile by type of *UGT1A1* polymorphism

	*UGT1A1*28 or UGT1A1*6* mutation			
	No mutation (*n* = 20)	Single (*n* = 11)	Double (*n* = 5)	*P*
Adverse events (no. of patient (%))				
Leukopenia grade 3 or 4				
First cycle	0 (0 %)	3 (27%)	2 (40%)	0.006[a]
All cycles	3 (15%)	3 (27%)	3 (60%)	0.046[a]
Neutropenia grade 3 or 4				
First cycle	1 (5%)	2 (18%)	2 (40%)	0.039[a]
All cycles	3 (15%)	3 (27%)	4 (80%)	0.008[a]
AUC ratio[b]	23.009	12.949	3.233	0.001[c]

Adverse events were assessed using National Cancer Institute Common Toxicity Criteria.

[a]Jonckheere–Terpstra test; [b]AUC ratio = $AUC_{SN\text{-}38G}/AUC_{SN\text{-}38}$; [c]Cochran–Armitage test.

polymorphisms are categorized and listed in **Figure 2**. Double mutations of *UGT1A1*28* and **6* (**6/*6* and **28/*6*) were detected in 5 of 36 patients (14%), and single mutations of *UGT1A1*28* or **6* were found in 11 of 36 patients (31%). No mutation was detected in 20 of 36 patients (55.6%). No *UGT1A1*28/*28* was found in homozygous patients.

Pharmacokinetic analyses were performed in the first cycle of treatment at a dosage of 100 mg/m², and the $AUC_{SN\text{-}38G}/AUC_{SN\text{-}38}$ ratios of the *UGT1A1*28* and **6* polymorphisms were compared (**Figure 2**). The $AUC_{SN\text{-}38G}/AUC_{SN\text{-}38}$ was 23.009 in the wild-type group. In the single-mutation group, the AUC ratios were 12.837 and 13.247 in **28* heterozygous and **6* heterozygous patients, respectively. In the double-mutation group, the ratios were 3.198 and 3.256 in **6* homozygous and **6/*28* heterozygous patients, respectively.

Table 4 Relationship between adverse events and pharmacokinetic profile during the first cycle of irinotecan treatment

Adverse event	Pharmacokinetic parameter	Spearman's rank correlation ρ (*P* value)
Leukopenia	CPT-11 AUC_{0-inf}	0.463 (<0.001)
	CPT-11 C_{max}	0.384 (0.001)
	SN-38 AUC_{0-inf}	0.542 (<0.001)
	SN-38 C_{max}	0.513 (<0.001)
Neutropenia	CPT-11 AUC_{0-inf}	0.449 (<0.001)
	CPT-11 C_{max}	0.314 (0.017)
	SN-38 AUC_{0-inf}	0.587 (<0.001)
	SN-38 C_{max}	0.59 (<0.001)

AUC, area under the time-concentration curve; C_{max}, peak plasma concentration; CPT-11, irinotecan.

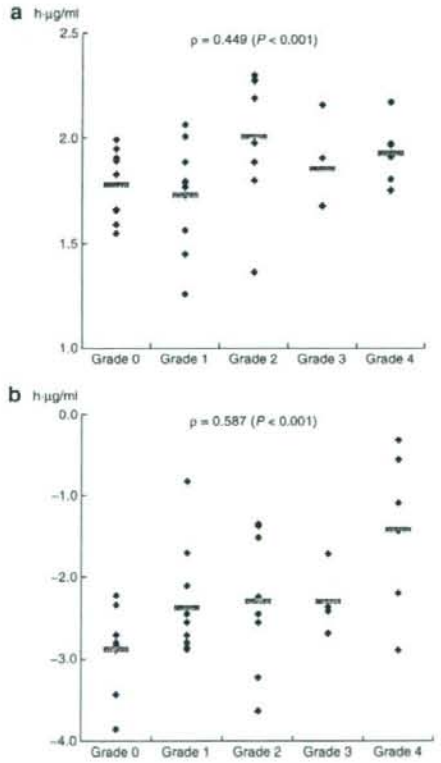

Figure 3 Correlation between neutropenia and pharmacokinetic profile: (**a**) CPT-11 AUC_{0-inf} and (**b**) SN-38 AUC_{0-inf}. The lines indicate geometric mean and the *y*-axis represents the log scale. AUC, area under the time-concentration curve.

The AUC_{SN-38G}/AUC_{SN-38} ratio was highest in the wild-type group, lower in the single-mutation group, and least in the double-mutation group. Although the number of patients was insufficient to establish statistical significance, the AUC_{SN-38G}/AUC_{SN-38} ratios of **6* heterozygous patients were nearly equivalent to those of **28* heterozygous patients, and those of **6* homozygous patients were nearly equivalent to those of **6/*28* heterozygous patients.

The association of *UGT1A1*28* and **6* polymorphisms with grade 3/4 hematological toxicity or AUC ratio was investigated during the first cycle of therapy. Significant correlations were observed between *UGT1A1*28* and **6* polymorphisms and AUC ratio ($P = 0.001$) and between *UGT1A1*28* and **6* polymorphisms and grade 3/4 hematological toxicity (**Table 3**). When the same association was examined through all cycles, a similar correlation between the incidence of grade 3/4 hematotoxicity and polymorphisms was observed (**Table 3**).

The relationship between adverse events and pharmacokinetic profile was further analyzed (**Table 4**). All five parameters correlated well with the frequency of grade 3/4 leukopenia and neutropenia ($P < 0.001$). The correlation between neutropenia and pharmacokinetic profile (CPT-11 AUC_{0-inf} and SN-38 AUC_{0-inf}) is shown in **Figure 3**. Both of these parameters correlated with neutropenia (CPT-11 AUC_{0-inf}: $\rho = 0.449$ ($P < 0.001$), SN-38 AUC_{0-inf}: $\rho = 0.587$ ($P < 0.001$)). The pharmacokinetic parameters of SN-38 appeared to correlate more significantly than those of CPT-11.

DISCUSSION

In this study, CPT-11 was administered on days 1 and 8 every 3 weeks in elderly patients (aged ≥70 years) with NSCLC, and the DLT, MTD, and RD were determined. The efficacy and safety of this regimen were investigated at the RD. In addition, the results were compared prospectively with the results of pharmacokinetic analysis and exploratory analysis of *UGT1A1* gene polymorphisms.

The results showed low antitumor effect for CPT-11 (response rate, 8.1%). The disease control rate was 21.6%. However, the TTP in this study was 132 days. This was longer than that observed in the phase III study we conducted.[13] Although the incidences of grade 3 or higher leukopenia, neutropenia, and anorexia were >20%, other adverse events occurred less frequently, and tolerability was acceptable. Also, the median number of treatment courses was four, and 22% of the patients were able to undergo prolonged treatment (more than eight courses). Almost all the doses of CPT-11 were administered as planned (dose intensity, 90%), and 25 patients were able to proceed to second-line therapy. As a result, an MST of 441 days was achieved. Because the MST was longer than predicted at the start of this study, the median follow-up time was also longer (440 days). These findings suggest that the regimen tested in this study is feasible and appropriate in elderly patients.

The high tolerability of this regimen contrasts with the results of a phase III comparative study of DOC monotherapy vs. VNR monotherapy in elderly patients (West Japan Thoracic Oncology Group Trial 9904)[9] conducted in Japan at around the same time. The response rate of 8.1% in our study was lower than that achieved with DOC monotherapy (22.7% in the West Japan Thoracic Oncology Group study). However, the survival time (14.3 months) was better in our study than that reported

in the West Japan Thoracic Oncology Group study. Moreover, the incidences of grade 3/4 neutropenia and leukopenia were 83 and 58%, respectively, with DOC,[9] which were higher than those in this study. These results indicate that this CPT-11 regimen should be considered as an option for first-line therapy in elderly patients with NSCLC.

To the best of our knowledge, this is the first prospective study with NSCLC patients that has explored the association between *UGT1A1* polymorphisms and the clinical effects of CPT-11 treatment. The $AUC_{SN\text{-}38G}/AUC_{SN\text{-}38}$ ratios were 23.009 in the wild-type group, 12.837 and 13.247 in the single-mutation group, and 3.198 and 3.256 in the double-mutation group, with the AUC ratio decreasing from wild-type to single-mutation to double-mutation groups. Furthermore, the individual AUC ratios in **6* heterozygous patients were similar to those in **28* heterozygous patients, and those in **6* homozygous patients were similar to those in **6/*28* heterozygous patients, although the number of patients in this study was too small to establish statistical significance.

Among the adverse events occurring during the first course of treatment, a correlation was observed between the incidence of grade 3/4 leukopenia or neutropenia and the AUC and peak plasma concentration of SN-38, as has been reported previously in relation to serious adverse reactions.[17–19] The results also showed that the incidence of grade 3/4 leukopenia and neutropenia was lowest in the wild-type group, higher in the single-mutation group, and highest in the double-mutation group of *UGT1A1*. We consider our classification of polymorphisms of *UGT1A1* as single-mutation and double-mutation appropriate.

The 100 mg/m^2 dose of intravenous CPT-11 on days 1 and 8 every 3 weeks was well tolerated in this prospective phase II study. These results suggest that this CPT-11 regimen should be considered as one of the options for first-line therapy in elderly patients with NSCLC. A phase III study has been scheduled to clarify the effect of *UGT1A1* mutations on response to CPT-11 therapy.

METHODS

Eligibility criteria. Chemotherapy- and radiotherapy-naive patients with histologically or cytologically proven stage IIIB/IV NSCLC were enrolled. Other eligibility criteria included age ≥70 years; measurable and assessable disease; Eastern Cooperative Oncology Group performance status of 0–1; an expected survival duration of ≥12 weeks; adequate bone marrow function (leukocyte count 4,000–12,000/mm^3; hemoglobin concentration ≥9.5 g/dl; platelet count ≥100,000/mm^3); serum creatinine at or below the institutional upper limits of normal level; total bilirubin level ≤1.5 mg/dl; and aspartate aminotransferase and alanine aminotransferase levels ≤100 IU. Laboratory tests were performed within 7 days of enrollment in the study. Exclusion criteria included the presence of symptomatic brain metastasis or apparent dementia; active concomitant malignancy; massive pleural effusion or ascites; active infection; severe heart disease or elevated electrocardiogram abnormality; uncontrolled diabetes mellitus; ileus; pulmonary fibrosis; diarrhea; or bleeding tendency. Written informed consent was obtained from all the participants. Institutional Review Board approval was obtained for the study protocol at each institution.

Treatment schedule. CPT-11 was administered intravenously over 1.5 h on days 1 and 8 of each 3-week cycle. In the phase I study, the starting dose, 60 mg/m^2 (level 1), was increased in 20-mg/m^2 increments to 100 mg/m^2 (level 3). The dosage of 100 mg/m^2 was used as the upper limit because this is the approved dosage for NSCLC in Japan. Dose escalation was carried out on the basis of toxicities encountered during cycle 1 of therapy. A cohort of at least three patients was treated at each dose level. If none of the first three patients experienced DLTs, the dose was escalated to the next level. If one of the three patients experienced DLTs, additional patients were enrolled at the same dose level to a total of at least six patients. The MTD was defined as the dose level below the one at which at least 33% of the patients experienced DLTs, defined as febrile neutropenia (neutrophil count <1,000/mm^3 and fever ≥38.5 °C), grade 4 neutropenia lasting >4 days, grade 3 or 4 leukopenia or anemia, grade 3 or 4 thrombocytopenia, or nonhematological toxicity (except electrolyte abnormality, nausea, anorexia, fatigue, or alopecia). A delay in the second CPT-11 administration of >7 days during the first cycle or >4 weeks between cycles was also categorized as a DLT. The RD was defined as the dose level below the MTD. If the MTD was not achieved at 100 mg/m^2, then 100 mg/m^2 was considered to be the RD because this is the dose that is used in clinical practice for nonelderly NSCLC patients.

Evaluation. In the phase II study, the efficacy and toxicity of CPT-11 monotherapy were evaluated at the RD. Tumor size was assessed by computed tomography at intervals of ≥6 weeks. Tumor response was categorized as CR, PR, stable disease, or progressive disease according to Response Evaluation Criteria in Solid Tumors.[23] Response rate was defined as CR plus PR. Disease control rate was defined as CR plus PR plus stable disease, including "shown no progression for 6 months." In order to be assigned a status of PR, the change in tumor size had to be confirmed by repeat assessments performed no less than 4 weeks after the criteria for response are first met. As for stable disease, it had to be confirmed by an assessment performed at least once after study enrollment but not earlier than 6 weeks. All tumor assessments were carried out by an investigator, and subsequently reviewed by the external response review committee. Toxicity was graded in accordance with the National Cancer Institute Common Toxicity Criteria, version 2 (ref. 24).

Pharmacokinetic assay. Venous blood for pharmacokinetic analysis was collected in sodium-heparinized and -evacuated tubes on day 1 of cycle 1, before CPT-11 infusion, at the end of infusion, and at 1, 2, 4, 7, and 24 h after infusion. The concentrations of unchanged CPT-11, SN-38, and SN-38G in plasma were determined using high-performance liquid chromatography,[25] and the $AUC_{0\text{-}inf}$ and peak plasma concentration were calculated using WinNonlin Version 4.1 (Pharsight, Mountain View, CA). The AUC ratio of SN-38G to SN-38 ($AUC_{SN\text{-}38G}/AUC_{SN\text{-}38}$) was calculated as a surrogate marker for *UGT1A1* activity involved in SN-38 glucuronidation.

UGT1A1 genotyping assay. *UGT1A1* polymorphisms were categorized into three groups: wild-type (**1/*1*), homozygous (**28/*28*, **6/*6*, **28/*6*), and heterozygous (**1/*28*, **1/*6*). Ando *et al.*[26] have reported that serious adverse events are associated with double-heterozygous (**28/*6*) as well as homozygous (**28/*28*, **6/*6*) polymorphisms. Sai *et al.*[27] also showed that the $AUC_{SN\text{-}38G}/AUC_{SN\text{-}38}$ ratio in patients with **28/*6* was similar to that in patients with **28/*28* and significantly lower than that in patients in the wild-type group.[22] On the basis of these two reports, we defined patients with *UGT1A1*28/*6*—along with those having the homozygous genotype of *UGT1A1*28/*28* or *UGT1A1*6/*6*—as the double-mutation group. Patients with the heterozygous genotype of either *UGT1A1*28* or *UGT1A1*6* were defined as the single-mutation group. Patients with no *UGT1A1*28* or *UGT1A1*6* mutations were defined as the no-mutation group.

Genomic DNA was extracted from the peripheral blood mononuclear cells of the 3 patients who received the RD in phase I and from 33 patients in phase II. One patient did not consent to analysis of *UGT1A1* genotype. For genotyping of *UGT1A1*6* polymorphism, products were amplified by direct PCR sequencing using the primer 5′-AAGTAGGAGAGGGCGAACC-3′ as described in ref. 26. Genotyping for the *UGT1A1*28* polymorphism was performed by subjecting amplified products to gel electrophoresis and determining the product size by migration rate, depending on the number of bases.

Statistical analysis. In the phase II study, the primary end point was the response rate. Secondary end points included survival time and 1-year survival rate. For achieving the ±15% confidence interval under an expected response rate of 25%, a total sample size of 33 patients was calculated as being required for the study.

The 95% confidence interval for treatment response was estimated according to *F*-distribution. Overall survival and cumulative TTP were determined using the Kaplan–Meier method. Overall survival time was calculated from the first day of therapy until the death of the patient or the last day that the patient was known to be alive. TTP was defined as the period from the first day of treatment to the date of (i) first evidence of any toxicity requiring discontinuation of protocol therapy, (ii) progressive disease, or (iii) death.

The Cochran-Armitage trend test was used for analyzing the trend of grade 3/4 adverse events across polymorphism types. Spearman's rank correlation test was used to assess the relationship between the grade of hematological toxicity and the pharmacokinetic profile in the first cycle. In this assessment, the grade according to the National Cancer Institute Common Toxicity Criteria was used as the continuous variable. The association between pharmacokinetic profiles and the type of polymorphism was assessed using the Jonckheere–Terpstra test. All analyses were performed using the SAS software, version 8.2 (SAS Institute, Cary, NC).

ACKNOWLEDGMENT

This study was supported by Yakult Honsha Co., Ltd.

CONFLICT OF INTEREST

The authors declared no conflict of interest.

1. World Health Organization: Revised Global Burden of Disease (GBD) 2002 Estimates of the World Health Organization, World Health Organization, 2004 <http://www.who.int/healthinfo/statistics/>. Accessed 6 August 2007.
2. National Institute of Population and Social Security Research: Population Projections for Japan: 2001–2050, National Institute of Population and Social Security Research, 2002 <http://www.ipss.go.jp/>. Accessed 6 August 2007.
3. World Health Organization: Reducing Risks, Promoting Healthy Life: The World Health Report 2002. (Geneva, Switzerland: World Health Reporting, World Health Organization, 2002).
4. Non-small Cell Lung Cancer Collaborative Group. Chemotherapy in non-small cell lung cancer: a meta-analysis using updated data on individual patients from 52 randomised clinical trials. *BMJ* **311**, 899–909 (1995).
5. Ohe, Y. *et al.* Randomized phase III study of cisplatin plus irinotecan versus carboplatin plus paclitaxel, cisplatin plus gemcitabine, and cisplatin plus vinorelbine for advanced non-small-cell lung cancer: Four-arm cooperative study in Japan. *Ann. Oncol.* **18**, 317–323 (2007).
6. Elderly Lung Cancer Vinorelbine Italian Study Group. Effects of vinorelbine on quality of life and survival of elderly patients with advanced non-small-cell lung cancer. *J. Natl. Cancer Inst.* **91**, 66–72 (1999).
7. Frasci, G. *et al.* Gemcitabine plus vinorelbine versus vinorelbine alone in elderly patients with advanced non-small-cell lung cancer. *J. Clin. Oncol.* **18**, 2529–2536 (2000).
8. Gridelli, C. *et al.* Chemotherapy for elderly patients with advanced non-small-cell lung cancer: the Multicenter Italian Lung Cancer in the Elderly Study (MILES) phase III randomized trial. *J. Natl. Cancer Inst.* **95**, 362–372 (2003).
9. Kudoh, S. *et al.* Phase III study of docetaxel compared with vinorelbine in elderly patients with advanced non-small-cell lung cancer: results of the West Japan Thoracic Oncology Group Trial (WJTOG 9904). *J. Clin. Oncol.* **24**, 3657–3663 (2006).
10. Mathijssen, R.H. *et al.* Clinical pharmacokinetics and metabolism of irinotecan (CPT-11). *Clin. Cancer Res.* **7**, 2182–2194 (2001).
11. Ma, M.K. & McLeod, H.L. Lessons learned from the irinotecan metabolic pathway. *Curr. Med. Chem.* **10**, 41–49 (2003).
12. Mathijssen, R.H. *et al.* Irinotecan pathway genotype analysis to predict pharmacokinetics. *Clin. Cancer Res.* **9**, 3246–3253 (2003).
13. Negoro, S. *et al.* Randomised phase III trial of irinotecan combined with cisplatin for advanced non-small-cell lung cancer. *Br. J. Cancer* **88**, 335–341 (2003).
14. Chabot, G.G. Clinical pharmacokinetics of irinotecan. *Clin. Pharmacokinet.* **33**, 245–259 (1997).
15. de Forni, M. *et al.* Phase I and pharmacokinetic study of the camptothecin derivative irinotecan, administered on a weekly schedule in cancer patients. *Cancer Res.* **54**, 4347–4354 (1994).
16. Iyer, L. *et al.* Genetic predisposition to the metabolism of irinotecan (CPT-11). Role of uridine diphosphate glucuronosyltransferase isoform 1A1 in the glucuronidation of its active metabolite (SN-38) in human liver microsomes. *J. Clin. Invest.* **101**, 847–854 (1998).
17. Innocenti, F. *et al.* Genetic variants in the UDP-glucuronosyltransferase 1A1 gene predict the risk of severe neutropenia of irinotecan. *J. Clin. Oncol.* **22**, 1382–1388 (2004).
18. Marcuello, E. *et al.* UGT1A1 gene variations and irinotecan treatment in patients with metastatic colorectal cancer. *Br. J. Cancer* **91**, 678–682 (2004).
19. Rouits, E., Boisdron-Celle, M., Dumont, A., Guérin, O., Morel, A. & Gamelin, E. Relevance of different UGT1A1 polymorphisms in irinotecan-induced toxicity: a molecular and clinical study of 75 patients. *Clin. Cancer Res.* **10** 5151–5159 (2004).
20. Beutler, E., Gelbart, T. & Demina, A. Racial variability in the UDP-glucuronosyltransferase 1 (UGT1A1) promoter: a balanced polymorphism for regulation of bilirubin metabolism? *Proc. Natl. Acad. Sci. USA* **95**, 8170–8174 (1998).
21. International HapMap Project. <http://www.hapmap.org/>.
22. Akaba, K. *et al.* Neonatal hyperbilirubinemia and mutation of the bilirubin uridine diphosphate-glucuronosyltransferase gene: a common missense mutation among Japanese, Koreans and Chinese. *Biochem. Mol. Biol. Int.* **46**, 21–26 (1998).
23. Patrick Therasse *et al.* New guidelines to evaluate the response to treatment in solid tumors. European Organization for Research and Treatment of Cancer, National Cancer Institute of the United States, National Cancer Institute of Canada. *J. Natl. Cancer Inst.* **92**, 205–216 (2000).
24. National Cancer Institute: Common Toxicity Criteria, version 2. (Division of Cancer treatment and Diagnosis, National Cancer Institute, Bethesda, MD, 1999). <http://www.fda.gov/cder/cancer/toxicityframe.htm>.
25. Kurita, A. & Kaneda, N. High-performance liquid chromatographic method for the simultaneous determination of the camptothecin derivative irinotecan hydrochloride, CPT-11, and its metabolites SN-38 and SN-38 glucuronide in rat plasma with a fully automated on-line solid-phase extraction system, PROSPEKT. *J. Chromatogr. B Biomed. Sci. Appl.* **724**, 335–344 (1999).
26. Ando, Y. *et al.* Polymorphisms of UDP-glucuronosyltransferase gene and irinotecan toxicity: a pharmacogenetic analysis. *Cancer Res.* **60**, 6921–6926 (2000).
27. Sai, K. *et al. UGT1A1* haplotypes associated with reduced glucuronidation and increased serum bilirubin in irinotecan-administered Japanese patients with cancer. *Clin. Pharmacol. Ther.* **75**, 501–515 (2004).

Carcinogenesis vol.29 no.11 pp.2139–2146, 2008
doi:10.1093/carcin/bgn200
Advance Access publication August 25, 2008

YAP1 is involved in mesothelioma development and negatively regulated by Merlin through phosphorylation

Toshihiko Yokoyama[1], Hirotaka Osada[1,2], Hideki Murakami[1], Yoshio Tatematsu[1], Tetsuo Taniguchi[1], Yutaka Kondo[1], Yasushi Yatabe[3], Yoshinori Hasegawa[4], Kaoru Shimokata[5], Yoshitsugu Horio[6], Toyoaki Hida[6] and Yoshitaka Sekido[1,*]

[1]Division of Molecular Oncology, Aichi Cancer Center Research Institute, 1-1 Kanokoden, Chikusa-ku, Nagoya 464-8681, Japan, [2]Department of Cellular Oncology, Nagoya University Graduate School of Medicine, 65 Tsurumai-cho, Showa-ku, Nagoya 466-8550, Japan, [3]Department of Pathology and Molecular Diagnostics, Aichi Cancer Center Hospital, 1-1 Kanokoden, Chikusa-ku, Nagoya 464-8681, Japan, [4]Department of Respiratory Medicine, Nagoya University School of Medicine, 65 Tsurumai-cho, Showa-ku, Nagoya 466-8550, Japan, [5]Department of Biomedical Sciences, College of Life and Health Sciences, Chubu University, 1200 Matsumoto-cho, Kasugai 487-8501, Japan and [6]Department of Thoracic Oncology, Aichi Cancer Center Hospital, 1-1 Kanokoden, Chikusa-ku, Nagoya 464-8681, Japan

*To whom correspondence should be addressed. Tel: +81 52 764 2993; Fax: +81 52 764 2993;
Email: ysekido@aichi-cc.jp

We previously reported the results of bacterial artificial chromosome array comprehensive genomic hybridization of malignant pleural mesotheliomas (MPMs), including two cases with high-level amplification in the 11q22 locus. In this study, we found that the *YAP1* gene encoding a transcriptional coactivator was localized in this amplified region and overexpressed in both cases, suggesting it as a candidate oncogene in this region. We analyzed the involvement of YAP1 in MPM proliferation, as well as its functional and physical interaction with Merlin encoded by the *neurofibromatosis type 2* (*NF2*) tumor suppressor gene, which is frequently mutated in MPMs. YAP1-RNA interference suppressed growth of a mesothelioma cell line NCI-H290 with *NF2* homozygous deletion, probably through cell-cycle arrest and apoptosis induction, whereas YAP1 transfection promoted the growth of MeT-5A, an immortalized mesothelial cell line. We also found that the introduction of *NF2* into NCI-H290 induced phosphorylation at serine 127 of YAP1, which was accompanied by reduction of nuclear localization of YAP1, whereas nuclear localization of a YAP1 S 127A mutant was not affected. Furthermore, results of immunoprecipitation and *in vitro* pull-down assays indicated a physical interaction between Merlin and YAP1. These results suggest that YAP1 is involved in mesothelial cell growth and that the transcriptional coactivator activity of YAP1 is functionally inhibited by Merlin through the induction of phosphorylation and cytoplasmic retention of YAP1. This is the first report of negative regulatory signaling from Merlin to YAP1 in mammalian cells. Future studies of transcriptional targets of YAP1 in MPMs may shed light on the molecular mechanisms of MPM development and lead to new therapeutic strategies.

Introduction

A malignant pleural mesothelioma (MPM) is a highly lethal neoplasm that is thought to develop from pleural mesothelial cells, with exposure to asbestos playing a crucial role in tumor development (1–4). Patients with an MPM are usually diagnosed at an advanced stage and the tumors are refractory to conventional therapeutic modalities; thus, their prognosis is very poor, even though advancements in chemotherapeutical modalities that combine cisplatin and antifolate, such as pemetrexed or raltitrexed, have been made (5,6). The long latency period between asbestos exposure and tumor appearance implies that multiple genetic changes are required for malignant transformation of mesothelial cells (7,8). Accumulated genetic studies have identified that tumor suppressor genes are crucial for MPM development, including frequent inactivation of $p16^{INK4a}/p14^{ARF}$ at 9p21 (9–11) and neurofibromatosis type 2 (*NF2*) at 22q12 (12–14). The *NF2* gene is responsible for NF2 syndrome (15) and encodes Merlin (also known as schwannomin), an ezrin/radixin/moesin family protein that has been shown to be involved in cytoskeletal dynamics, growth factor receptor signaling and cell adhesion (16,17).

To further elucidate the alterations of oncogenes and tumor suppressor genes responsible for MPM development, we previously carried out bacterial artificial chromosome (BAC) array comprehensive genomic hybridization (CGH) analyses of MPM specimens from a total of 22 individuals and reported several distinct chromosomal alterations including high copy amplification of 11q22 (18). In the present study, we found that the *YAP1* gene, which was originally cloned as a partner of Yes kinase (19), resides within the 11q22 amplification region and that YAP1 is involved in mesothelial cell growth. Furthermore, we found that YAP1 activity may be negatively regulated via Merlin signaling in mesothelial cells. To our knowledge, this is the first known report of the existence of negative regulatory signaling from Merlin to YAP1 in mammalian cells, which may play a crucial role in growth regulation of mesothelial cells and development of malignant mesothelioma.

Materials and methods

Array CGH analysis and quantitative polymerase chain reaction analyses of copy number and expression

Genome-wide array CGH analysis of 22 individual MPMs using microarrays with 2304 BAC and P-1 phage-derived artificial chromosome clones covering the whole human genome at a resolution of roughly 1.3 Mb was previously reported (18). To determine the precise copy numbers within the amplification, quantitative polymerase chain reaction (PCR) using custom TaqMan probes (Applied Biosystems, Foster City, CA) corresponding to the genomic sequences of seven genes (*PGR, TRPC6, ANGPTL5, YAP1, BIRC2, MMP13* and *AB08258*) dispersed within the 3 Mb region were designed and used together with TaqMan PCR master mix (Applied Biosystems) and an ABI7500 system (Applied Biosystems), according to the manufacturer's instructions. The copy number of the leucine-rich repeat containing the *4C* gene (also called *NGLI*) localized at 11p12 was used as a control. To examine the expression of genes within each amplification, TaqMan expression probes (Applied Biosystems) for *ANGPTL5, YAP1, BIRC2* and *BIRC3* were used, and quantification was performed as above.

Construction of RNA interference vectors and expression vectors

To construct RNA interference (RNAi) vectors, short hairpin (sh) oligonucleotides were inserted into a plasmid containing the U6 promoter and a puromycin-resistant gene (20). Two sh oligonucleotides were designed for two different sequences within the YAP1 open reading frame (YAP1-sh1, GGCCATGCTGTCCCAGATGAAT and YAP1-sh2, GGAGATGGAATGAACATAGAAT). In addition, control vectors, YAP1-scr1 and green fluorescent protein (GFP)-sh, were constructed using oligonucleotides with scrambled sequences for YAP1-sh1 (GGCTGCCATTCGCGACATGAAT) and GFP open reading frame (GFP-sh, GCAAGCTGACCCTGAAGTTCA). YAP1 cDNA was purchased from OriGene (Rockville, MD) and inserted into pcDNA (Invitrogen, Carlsbad, CA) and pEGFP-C1 (Clontech, Mountain View, CA) vectors. The phosphorylation-defective mutant YAP1 was constructed by *in vitro* mutagenesis at codon 127 from serine to alanine (S 127A), as the phosphorylation of serine 127 was reported to induce an interaction between 14-3-3 and cytoplasmic retention (21). *NF2* cDNA was amplified with reverse transcription–PCR and cloned into pcDNA (Invitrogen) and the lentivirus vector pLentiLox3.7. The *Na(+)/H(+) exchanger regulatory factor 1 (NHERF1)/ezrin/radixin/moesin-binding phosphoprotein 50 kD* gene expression constructs

Abbreviations: BAC, bacterial artificial chromosome; CGH, comprehensive genomic hybridization; EGFP, enhanced green fluorescent protein; GST, glutathione S-transferase; MPM, malignant pleural mesothelioma; NF2, neurofibromatosis type 2; NHERF1, Na(+)/H(+) exchanger regulatory factor 1; PCR, polymerase chain reaction; RNAi, RNA interference; SDS, sodium dodecyl sulfate; sh, short hairpin.

were kindly provided by Dr Maria-Magdalena Georgescu (University of Texas M. D. Anderson Cancer Center) and Dr Martha C. Nowycky (University of Medicine and Dentistry of New Jersey).

Cell culture and colorimetric and flow cytometry analyses

A malignant mesothelioma cell line (NCI-H290), a gift from Dr Adi F. Gazdar (University of Texas Southwestern Medical Center), and a non-malignant mesothelial cell line (MeT-5A), purchased from American Type Culture Collection (Rockville, MD), were cultured as described previously (18). YAP1-RNAi vectors were transfected into NCI-H290 or MeT-5A cells using Lipofectamine 2000 (Invitrogen). For cell proliferation analysis, transfected cells were treated with puromycin at 1 μg/ml for 10 days, then stained using TetracolorOne (Seikagaku, Tokyo, Japan), after which absorbance was determined at 450 nm. For analysis of the cell cycle and sub-G_1 population, transfected cells were treated with puromycin at 1 μg/ml for 24 h, after which the culture medium and dead cells were removed. Residual and viable cells were further cultured without puromycin for 24 h, then harvested and stained with propidium iodide for flow cytometry analysis, as described previously (20).

Immunoblotting analysis

For preparation of nuclear and cytoplasmic fractions, cells were incubated in hypotonic buffer with 0.5% NP-40, then the nuclei were pelleted using a brief centrifugation, as described previously (22). For immunoblotting analysis, after harvesting the cells with lysis buffer, protein concentration was determined with a DC Protein assay kit (Bio-Rad, Hercules, CA). The same amounts of protein samples were applied to sodium dodecyl sulfate (SDS)–polyacrylamide gel electrophoresis, then electrotransferred to Immobilon-P polyvinylidene difluoride membranes. Each membrane was incubated with anti-V5-tag (Invitrogen) for V5-tagged NF2, anti-YAP1 (Cell Signaling and Abnova, Taipei, Taiwan) and anti-S 127 phospho-YAP1 (Cell Signaling, Danvers, MA) antibodies, then visualized using an ECL detection kit (GE Healthcare, Amersham Place, UK).

Immunofluorescent microscopic analysis

NCI-H290 cells were transfected with expression vectors for the enhanced green fluorescent protein (EGFP)-fused YAP1 wild-type or S 127A mutant together with V5-tagged NF2 or an empty vector and cultured on cover glass slides. The transfected cells were then fixed, permeabilized and incubated with anti-V5 and Alexa Fluor568-conjugated anti-mouse antibodies and examined with a confocal microscope (LSM510, Carl Zeiss MicroImaging GmbH, Jena, Germany).

Immunoprecipitation and in vitro pull-down assays

For immunoprecipitation analyses, 293T cells were transfected with the EGFP-fused wild-type or S 127A mutant YAP1 constructs together with V5-tagged NF2 or an empty vector. Immunoprecipitates of lysates transfected with the anti-V5 antibody were subjected to SDS–polyacrylamide gel electrophoresis and immunoblotting with various antibodies.

For *in vitro* pull-down assays, human NF2 full-length cDNAs were inserted into a pGEX-KG vector (Amersham Pharmacia Biotech, Uppsala, Sweden) to express bacterial glutathione S-transferase (GST)–Merlin fusion protein. GST–Merlin or GST-alone proteins were purified from the transformed bacterial lysates by incubation with glutathione sepharose beads (GE Healthcare). The YAP1 protein expressed with an *in vitro* transcription/translation system (Promega, Madison, WI) or cell lysate of 293T transfectants were incubated with beads containing 3 μg of immobilized GST-alone or GST–Merlin fusion proteins for 3 h at 4°C, then washed four times. Proteins bound to GST proteins were eluted by boiling in SDS sample buffer, then separated by SDS–polyacrylamide gel electrophoresis and immunoblotted with various antibodies.

Results

Precise mapping of 11q22 amplification region in malignant mesotheliomas

We previously reported the results of genome-wide array CGH analyses of MPMs derived from 22 individuals, in which it was notable that two primary MPM cases (KD1033 and KD 1041) showed two discrete and significant high-level amplifications in the chromosome 1p32 and 11q22 regions (18). Since we demonstrated that the *JUN* proto-oncogene resided in the 1p32 amplification region, whose expression was shown to be induced by asbestos exposure in rat pleural mesothelial cells (23) and whose amplification was recently demonstrated in aggressive sarcomas (24), we speculated that the 11q22 amplification region may also harbor an important target gene whose overexpression is involved in MPM cell growth. To identify the target gene, we precisely determined the extent of the amplified regions from these two cases that were overlapped and bounded by RP11-40B14 and RP11-652L13 BAC probes, with only two BAC probes (RP11-203C2 and RP11-864G5) included between them (Figure 1A). With quantitative PCR analysis using TaqMan probes, the copy numbers of seven genes (*PGR*, *TRPC6*, *ANGPTL5*, *YAP1*, *BIRC2*, *MMP13* and *AB08258*) which dispersed within the 3-Mb-long region were investigated. As expected, both tumors were shown to carry high copy numbers of the *ANGPTL5*, *YAP1*, *BIRC2* and *MMP13* genes, while no gains were detected in *TRPC6* and *AB08258* genes, indicating that the extent of the common amplification region was ~1 Mb in length including 14 candidate genes (Figure 1B). In addition, comparing with each gene amplification level carefully, both *ANGPTL5* and *YAP1* showed about a 2-fold greater increase in copy numbers than *BIRC2* and *MMP13* in KD1033, while each amplification level of the four genes was similar in KD1041 (Figures 1B and 2C). This result suggested that the amplification of the centromeric half region including *ANGPTL5* and *YAP1* might be more important than that of telomeric region including the *BIRC2* and *MMP* cluster during the development of those MPMs, at least in KD1033.

Overexpression of YAP1 and BIRC2 in malignant mesotheliomas

To determine which gene residing in the 1 Mb amplification region was the most responsible for the development of these MPM cases, we next studied the expression levels of each gene using real-time reverse transcription–PCR analysis. Among the four genes in the centromeric half amplification region, *ANGPTL5*, *YAP1* and *BIRC2* were overexpressed in KD1033, whereas *YAP1*, *BIRC2* and *BIRC3* in KD1041, indicating that only *YAP1* and *BIRC2*, but not *ANGPTL5* or *BIRC3*, were commonly overexpressed in these tumors (Figure 2A). These results strongly suggest that the most probable target genes in this amplification region are *YAP1* and *BIRC2*. Meanwhile, we also examined the expression levels of several *MMP* cluster genes, but did not detect any overexpression, again suggesting that amplification of the telomeric half region was not significant (data not shown). The immunohistochemical staining results also clearly demonstrated the overexpression of YAP1 in KD1033 (Figure 2B, left panel), though normal pleural mesothelial cells did not show any YAP1 signals (arrowheads in Figure 2B, right panel).

Next, to determine whether other MPMs not shown to have clear amplification in BAC/P-1 phage derived artificial chromosome array CGH analysis may also have a more confined amplification or deregulation of the *YAP1* and *BIRC2* genes, we examined the copy numbers as well as expression levels of these genes using 12 additional primary MPM cases (Figure 2C and D) and 13 MPM cell lines (data not shown). However, amplification of these genes in these MPM specimens and cell lines was not detected, except for KD1033 and KD1041, nor was there significant upregulation of the others observed (Figure 2C and D). These results suggest that even though significant overexpression of the *YAP1* and *BIRC2* genes can occur, amplification of these genes is a relatively infrequent event in MPMs.

Involvement of YAP1 in mesothelial cell proliferation

To determine cancer-promoting roles of these genes in mesothelioma cells, we first focused on the *YAP1* gene since its positive role has also been suggested in other malignancies (25,26). We synthesized two YAP1-RNAi vectors, YAP1-sh1 and YAP1-sh2, to suppress endogenous YAP1 expression, a scramble control vector, YAP1-scr1, and a GFP-RNAi vector, GFP-sh. These vectors were transfected into MPM cell line NCI-H290 cells, and expression levels of endogenous YAP1 protein were examined. Both YAP1-RNAi vectors effectively reduced the expression levels of YAP1 to 30 and 10%, respectively, whereas the control vectors (GFP-sh and YAP1-scr1) did not demonstrate any suppression (Figure 3A). We then studied the effects of YAP1-RNAi on cell proliferation of mesothelioma. Both YAP1-RNAi vectors demonstrated significant suppression of cell proliferation, with YAP1-sh2 showing complete abolition of cell proliferation (Figure 3B). Flow cytometry analysis revealed that cells transfected by YAP1-sh2 showed G_1 arrest and induction of a sub-G_1 population

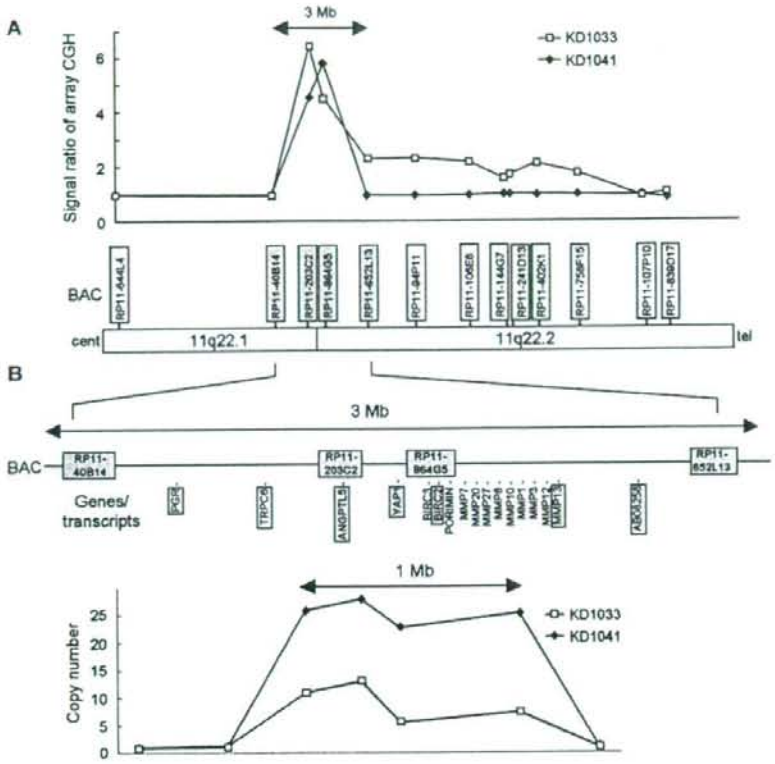

Fig. 1. Mapping of amplified region of 11q22 locus in two MPM cases. (A) Details of array-CGH results of 11q22 amplification in two MPM cases. The signal ratios from array CGH analyses of two primary MPM cases (KD1033 and KD 1041) were plotted for all BAC clones based on chromosome position, and the results indicated discrete and significant amplifications at the 11q22 region. Amplifications in both cases were similar within a 3-Mb-long region, which was bounded by RP11-40B14 and RP11-652L13, and included only two BAC probes (RP11-203C2 and RP11-864G5), represented by open squares and closed diamonds, respectively. (B) Copy number analyses using quantitative PCR with TaqMan probes. Genes and registered transcripts within the 3-Mb-long region are shown. To further determine the boundaries of the amplified regions, the copy numbers of seven genes (*PGR, TRPC6, ANGPTL5, YAP1, BIRC2, MMP13* and *AB08258*, indicated by boxes) were investigated using TaqMan probes. Four genes (*ANGPTL5, YAP1, BIRC2* and *MMP13*) showed high copy numbers in the two MPM cases, suggesting that both carried quite similar 1-Mb-long amplifications.

and those by YAP1-sh1 a moderate induction of the sub-G_1 population (Figure 3C and D). In contrast, the control vectors did not show any growth-suppressive effect.

Furthermore, we transfected a YAP1 expression vector into the immortalized mesothelial cell line MeT-5A to figure out whether YAP1 has growth-promoting activity in mesothelial cells. YAP1 overexpression moderately supported cell proliferation in a low-serum condition of 1% fetal calf serum, whereas it did not demonstrate clear promotion of cell proliferation in the usual condition (fetal calf serum 5%) (Figure 3E).

Functional interaction between YAP1 and Merlin

Since the Merlin-encoding *NF2* gene is frequently altered in MPMs, and the Merlin–Hippo–Warts pathway in *Drosophila* is known to negatively regulate Yorkie, the *Drosophila* ortholog of YAP1 through its phosphorylation (27), the results shown above strongly suggested that Merlin, as an upstream molecule, may functionally interact with and also suppress YAP1 in human mesothelial cells. In order to confirm this hypothesis, we cotransfected the *NF2* and *YAP1* expression vectors into NCI-H290 cells carrying a homozygous deletion of the *NF2* gene and studied whether exogenous Merlin has an effect on the phosphorylation status of YAP1 using the antibody against phosphorylated serine 127 (S 127) of YAP1, a critical phosphorylation site that has been indicated to induce inactivation of YAP1 as transcription coactivator through the induction of cytoplasmic retention (21). We found that cotransfection significantly induced the phosphorylation of YAP1 at S 127 (Figure 4A). To further demonstrate YAP1 S 127 phosphorylation by the activated form of Merlin, we also synthesized lentivirus vectors for full-length NF2 and truncated four-point-one/ezrin/radixin/moesin (FERM)-NF2 which translates 340 amino acids of the amino terminal and transfected into NCI-H290 cells. As expected, S 127 phosphorylation of YAP1 was induced by full-length NF2 in a dose-dependent manner, but not with truncated FERM-NF2 (Figure 4B).

Next, we determined whether phosphorylation of YAP1 protein induced its cytoplasmic localization, resulting in YAP1 inactivation as a transcriptional coactivator. We transfected NCI-H290 cells with EGFP-fused wild-type or S 127A mutant *YAP1*, together with *NF2* or an empty vector, and studied the subcellular localization using immunoblotting (Figure 4C) and immunofluorescence (Figure 4D). Immunoblotting of fractionated lysates, also depicted as a bar graph in the figure, clearly showed that wild-type phospho-YAP1 was scarcely detectable in the nuclear fractions, whereas the total YAP1 protein was localized in both the nucleus and cytoplasm (Figure 4C). In addition, the nuclear proportion of mutant YAP1 was higher than that of wild-type YAP1 (Figure 4C). These results suggested that

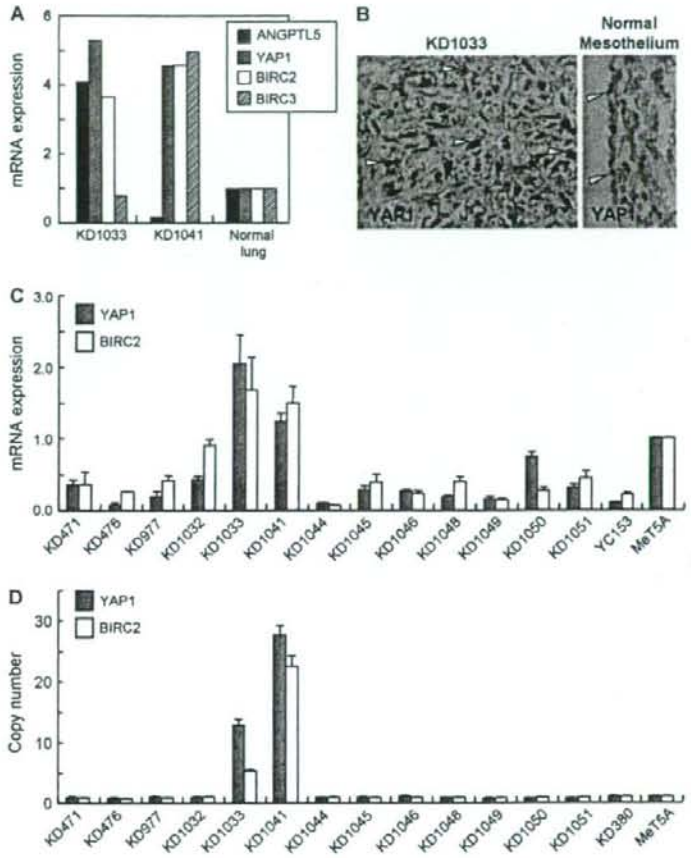

Fig. 2. Alterations of copy number and expression of *YAP1* and *BIRC2*. (**A**) Expression analyses of the *ANGPTL5*, *YAP1*, *BIRC2* and *BIRC3* genes indicated that *YAP1* and *BIRC2* were overexpressed in common in both MPM cases with amplification. (**B**) Immunohistochemical staining of YAP1. Immunohistochemical analysis clearly demonstrated overexpression and nuclear accumulation of YAP1 in KD1033 (left panel), whereas normal pleural mesothelial cells did not show any YAP1 signals (arrowheads, right panel). (**C**) Expression analysis in primary MPM cases. In an examination of 14 primary MPM cases and the normal mesothelial cell line MeT-5A, the two MPM cases showed the greatest amount of upregulated expressions of the *YAP1* and *BIRC2* genes with amplification. (**D**) Copy number analysis of primary MPM cases. In an examination of 14 MPM cases and the normal mesothelial cell line MeT-5A, only the two MPM cases demonstrated amplification of the *YAP1* and *BIRC2* genes.

phosphorylation negatively regulates nuclear localization and transcriptional activity of YAP1 protein. Although Merlin induced phosphorylation of YAP1, the nuclear proportion of wild-type total YAP1 was not significantly reduced, probably because of the existence of YAP1-alone transfectants.

Next, we performed immunofluorescence to further confirm that the subcellular localization of YAP1 protein is dependent on phosphorylation induced by Merlin. NCI-H290 cells were transfected with an EGFP-fused wild-type or S 127A mutant *YAP1* construct, together with *NF2* or an empty vector. Both the wild-type and mutant YAP1 proteins were found to be localized in both the nuclei and cytoplasm of the empty vector-cotransfected cells (Figure 4D). In contrast, cotransfection of the *NF2* vector clearly reduced nuclear localization of the wild-type YAP1 proteins, but not the mutant YAP1 protein. In addition, immunohistochemical staining of nuclear accumulation of YAP1 in the MPM case with YAP1 gene amplification (arrowheads in Figure 2B, left panel) also supported the idea that YAP1 localization in nuclei of the tested cell lines was not due to an artificial event.

Physical interaction between YAP1 and Merlin

Since these transfection experiments indicated a functional relationship between Merlin and YAP1, we next studied whether these molecules physically interact with each other. We immunoprecipitated Merlin from the lysates of 293T cells that were cotransfected with *NF2* and/or *YAP1* expression vectors and then investigated whether YAP1 could be coprecipitated with Merlin (Figure 5A). The results clearly demonstrated the coprecipitation of YAP1 with Merlin, indicating a physical interaction between them. Interestingly, the anti-phospho-YAP1 antibody did not show any signals, while the S 127A mutant YAP1 also interacted with Merlin as did wild-type YAP1 (Figure 5A), suggesting that Merlin may also interact with unphosphorylated YAP1.

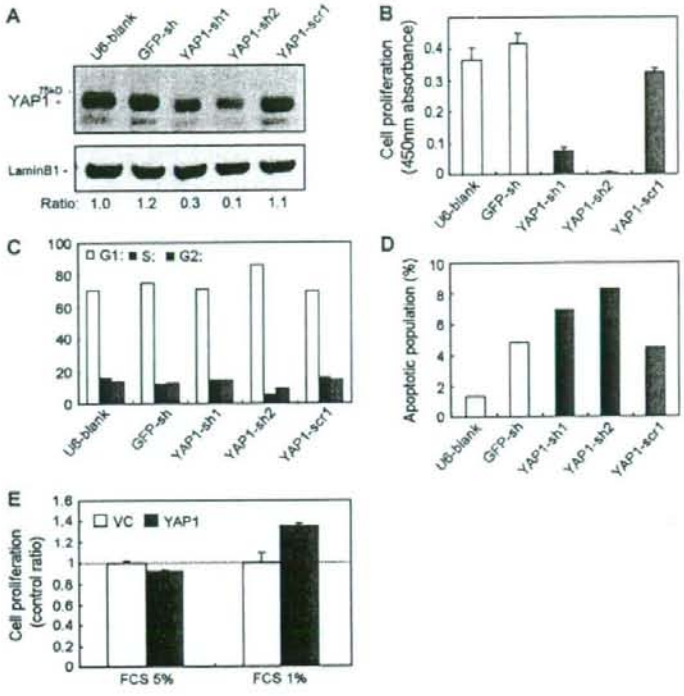

Fig. 3. Involvement of YAP1 in cell proliferation. (**A**) Knockdown of endogenous YAP1 in MPM cell line NCI-H290. Both YAP1-RNAi vectors, YAP1-sh1 and YAP1-sh2, showed effective suppression of the level of YAP1 protein, whereas the control vectors, GFP-sh and YAP1-scr1, showed no inhibition. (**B**) Inhibition of NCI-H290 proliferation by YAP1-RNAi. Colorimetric assay results demonstrated that both the YAP1-sh1 and YAP1-sh2 vectors induced significant suppression of cell proliferation. YAP1-sh2 inhibited proliferation to a greater degree as compared with YAP1-sh1, consistent with the RNAi effect. (**C**) Cell-cycle arrest by YAP1-RNAi. YAP1-sh2 clearly induced G_1 arrest of NCI-H290 cells. (**D**) Induction of sub-G_1 population by YAP1-RNAi. The sub-G_1 population of NCI-H290 cells was induced by both YAP1-RNAi vectors, though induction by YAP1-sh2 was greater. (**E**) Promotion of MeT-5A cell proliferation by YAP1 overexpression. Although YAP1 overexpression did not show a clear effect in the usual condition [fetal calf serum (FCS) 5%], YAP1 overexpression moderately promoted cell proliferation in the low-serum condition (FCS 1%).

To further confirm the physical interaction between YAP1 and Merlin, we prepared GST-alone or GST—Merlin-bound glutathione beads and then performed *in vitro* pull-down assays (Figure 5B). First, we conducted a pull-down assay using *in vitro*-translated YAP1 protein; however, no association between YAP1 and GST–Merlin was detected (Supplementary Figure 1), which suggested that YAP1 was not directly associated with Merlin. Next, we performed a pull-down assay using the lysate of 293T cells transfected with the YAP1 expression vector, as we considered that the cell lysate possibly contained endogenous molecules that could bridge YAP1 and Merlin. The pull-down assay using the 293T cell lysate clearly demonstrated that YAP1 was associated with GST–Merlin (Figure 5B, lane 2). In addition, we also studied the effects of NHERF1/ezrin/radixin/moesin-binding phosphoprotein 50 kD because it was reported to be associated with YAP1 (28) as well as with Merlin (29), and we considered that it might bridge the YAP1 and Merlin proteins. However, NHERF1 seemed unable to enhance the YAP1–Merlin association, though NHERF1 bound to GST–Merlin (Figure 5B, lane 4). These results indicate that YAP1 is indirectly associated with Merlin, probably through an endogenous bridging molecule other than NHERF1.

Discussion

In the present study, we demonstrated that the *YAP1* gene is localized in the high-level 11q22 amplification region, which we previously reported in a study of two cases with MPMs, and that *YAP1* together with *BIRC2* are overexpressed in these tumors. We also found that upregulation of YAP1 induced mesothelial cell proliferation, whereas its downregulation inhibited that proliferation. Furthermore, Merlin-dependent phosphorylation inhibits the nuclear localization of YAP1, which might result in inactivation of YAP1 transcriptional activity.

Amplifications at the 11q22 locus have been reported for several different types of human cancer (25,30–33). Amplifications at mouse chromosome 9qA1, the syntenic region of human chromosome 11q22, have also been shown in mouse mammary and liver cancers (25,26). Furthermore, during preparation of the present manuscript, MPM cell lines carrying chromosomal gain at the 11q22 locus were also reported (34). These findings, together with our previous array CGH analysis on malignant mesotheliomas, suggested a significant role for 11q22 amplification in carcinogenesis. In the present study, we demonstrated that, among the several candidate oncogenes at the 11q22 amplification region, both the *YAP1* and *BIRC2* genes were commonly overexpressed in the two MPM tissues, suggesting that *YAP1* and *BIRC2* were the most likely target genes. We focused on YAP1 primarily because previous reports have suggested its oncogenic activity of YAP1 (25,26). *In vitro* transfection assay that utilized knockdown or overexpression of YAP1 indicated that YAP1 promotes growth of mesothelial lineage cells, and cotransfection experiments strongly suggested that Merlin inhibits the transcriptional activator activity of YAP1 through induction of phosphorylation and inhibition

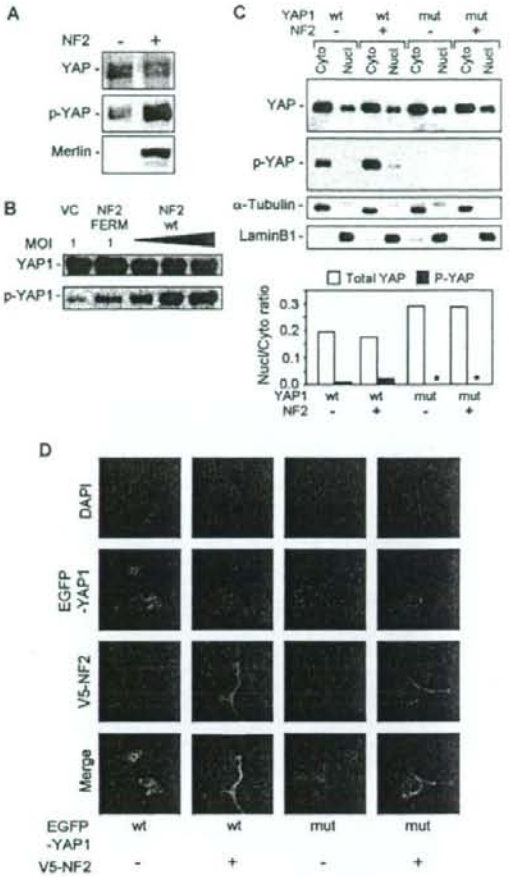

Fig. 4. Functional interaction between YAP1 and Merlin. (**A** and **B**) Induction of YAP1 phosphorylation by Merlin. (**A**) NF2-null NCI-H290 cells were transfected with YAP1 and NF2 expression vectors. Cotransfection of NF2 significantly induced phosphorylation of the YAP1 S 127 residue. (**B**) Either full-length or truncated NF2 was introduced into NCI-H290 cells with a lentivirus. Phosphorylation of YAP1 was induced by the full-length NF2 lentivirus in a dose-dependent manner, whereas the truncated NF2 FERM lentivirus did not have any clear effect. (**C**) Immunoblotting of cytoplasmic and nuclear fractions. NCI-H290 cells were transfected with wild-type (wt) or phosphorylation-defective S 127A mutant (mut) YAP1 and NF2 expression vectors. Immunoblots of nuclear and cytoplasmic fractions of transfectants clearly showed that phospho-YAP1 was mainly localized in the cytoplasm, as detected by the anti-S 127 phospho-YAP1 antibody, though total YAP1 was localized in both the nucleus and cytoplasm. In addition, the nuclear/cytoplasmic ratio of YAP1 and phospho-YAP1 proteins was measured with a densitometer and indicated with a bar graph, which clearly demonstrates the tight cytoplasmic retention of wild-type phospho-YAP1 protein. No signals were detected in mutant YAP1 transfectants with the anti-phospho-YAP1 antibody (asterisks). Results of immunoblotting with antibodies against α-tubulin and nuclear laminB1 indicated that proper fractionation occurred. (**D**) Reduction of YAP1 nuclear localization by NF2. NCI-H290 cells were transfected with expression vectors of the EGFP-fused wild-type (wt) or S 127A mutant (mut) YAP1, together with the vector control or V5-tagged NF2. Both the wild-type and mutant YAP1 proteins localize in both the nuclei and cytoplasm of H290 cells. Cotransfection of NF2 reduced nuclear localization of wild-type YAP1, whereas the localization of mutant YAP1 was not affected by NF2.

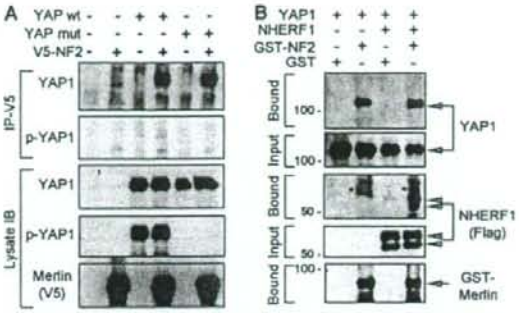

Fig. 5. Physical interaction between YAP1 and Merlin. (**A**) Immunoprecipitation: 293T cells were transfected with V5-tagged *NF2* and/or *YAP1* expression vectors, then Merlin was immunoprecipitated with the anti-V5 antibody and coprecipitation with YAP1 was studied. Both wild-type and S 127A mutant YAP1 were coprecipitated with Merlin. The anti-phospho-YAP1 antibody did not show any clear signals. (**B**) *In vitro* pull-down assay. Cell lysates of 293T cells were transfected with a *YAP1* or *NHERF1* vector, then incubated with GST-alone or GST—Merlin-bound beads. Immunoblots of bead-bound proteins (Bound) and the initial cell lysates (Input) are shown. Both YAP1 and NHERF1 proteins bound to GST–Merlin, though NHERF1 did not enhance the association of YAP1 with GST–Merlin. In the immunoblot of bound NHERF1, non-specific bands are indicated by asterisks.

of nuclear localization. To our knowledge, the present results are the first to show that YAP1 is regulated by Merlin through induction of phosphorylation, indicating that YAP1 is a downstream effector of Merlin tumor suppressor signaling in mammals. Our findings also suggest that YAP1 may play a crucial role in MPM development because Merlin tumor suppressor signaling is frequently altered in those tumors.

Recent genetic and biochemical analyses of *Drosophila* demonstrated that cell proliferation and organ size are negatively regulated by a kinase cascade of Hippo and Warts (also called Lats) and that two membrane-associated proteins, Merlin and Expanded, function upstream of this kinase cascade (35). Yorkie, the *Drosophila* ortholog of YAP1, is a critical target of the growth-inhibitory Hippo–Warts/Lats kinase cascade and a potential oncogene because its overexpression induces tissue overgrowth and apoptosis inhibition through the transactivation of cycE and diap1 expression (27,36). *Drosophila* rescue experiments also indicated evolutionary conservation of the signaling components, that is the mammalian *LATS1*, *MOB1*, *MST2* and *YAP* genes, which are orthologs of the *Drosophila Warts*, *Mats*, *Hippo* and *Yorki* genes, respectively. During the preparation of this manuscript, Zhao *et al.* (37) clearly demonstrated that the S 127 phosphorylation of YAP1 was catalyzed by LATS1 and that YAP1 inactivation plays significant roles in cell contact inhibition and tissue growth regulation. However, the signaling pathway from Merlin to YAP1 has not been clearly demonstrated in mammalian cells.

YAP1 has been reported to bind to and regulate the activities of various transcriptional regulators, including p73, RUNX2, ERBB4, and several TEA domain/transcription enhancer factor-type transcription factors, and also shown to function as an oncogene in mammals (25,26), possibly through an association with RUNX2 (38,39) and ERBB4 (19,40). YAP1 is phosphorylated at S 127, leading to its association with 14-3-3, which sequestrates YAP1 in the cytoplasm and inhibits its coactivator activity (21,41). The present results demonstrated that Merlin induces phosphorylation of YAP1 S 127 and inhibits its nuclear localization. Merlin–YAP1 signaling is conceivable, because, based on conserved *Drosophila* signaling, Merlin may activate the MST2–LATS1 kinase cascade, while it also appears to bind to unphosphorylated YAP1 protein.

YAP1 has also been reported to promote apoptosis through an association with p73 (21,42,43). In addition, a recent report demonstrated that LATS1 was activated by tumor suppressor RASSF1A to phosphorylate YAP1 and promote nuclear localization of the YAP1–p73 complex, resulting in apoptosis induction (44). Therefore, YAP1 may promote both cell growth and apoptosis, depending on the associated transcription factors. In this context, overexpression of *BIRC2* and *BIRC3* genes, which colocalize at 11q22 and encode apoptosis inhibitors, might be essential for exhibition of the oncogenic activity of YAP1 in cancers with 11q22 amplification, with our cases being consistent with this idea.

The *NF2* gene is frequently inactivated in MPMs, indicating that downregulation of Merlin signaling is essential for MPM development. The antiproliferative effect of Merlin in *NF2*-deficient mesothelioma cells has been suggested to be induced by repressing cyclin D1 expression (45), attenuating focal adhesion kinase phosphorylation (46) or interacting with NF2-associated guanosine triphosphate-binding protein (47). *Nf2*(+/−) mice exposed to asbestos exhibit accelerated formation of highly malignant mesothelial tumors (48,49). In addition, in a recent study, conditional knockout mouse models developed by inactivating *Nf2* together with $p16^{Ink4a}/p19^{Arf}$, *p53* or both, developed malignant mesotheliomas at a high incidence, supporting the notion that *Nf2* inactivation is important for the pathogenesis of these tumors (50). Our results revealed that the *YAP1* gene can also be an activating target for a subset of MPMs, which was coincidentally found to be a downstream effector of the Merlin cascade. However, though YAP1 may be important in the subset of MPM with 11q22 amplification, its relevance in the vast majority of MPM cases is unknown at present. Therefore, precise analysis of tumor suppressor signaling in NF2–MST–WARTS/LATS–YAP1 is needed to shed light on the molecular mechanisms of MPM development in greater detail. Preliminary analysis of immunohistochemical staining of YAP1 revealed overexpression and nuclear localization of YAP1 in a subset of MPM cases, indicating the frequent involvement of YAP1 in MPM development. Nevertheless, the present results provide new insights into genetic alterations in MPMs and clues for development of a new molecular target therapy for patients with these tumors.

Supplementary material

Supplementary Figure 1 can be found at http://carcin.oxfordjournals.org/

Funding

Special Coordination Fund for Promoting Science and Technology from the Ministry of Education, Culture, Sports, Science and Technology (H18-1-3-3-1); Grant-in-Aid for Scientific Research from Japan Society for the Promotion of Science (18390245).

Acknowledgements

We thank Dr Masashi Kondo and Dr Noriyasu Usami for their helpful comments and special encouragement. Dr Maria-Magdalena Georgescu and Dr Martha C. Nowycky for the constructs, and Dr Adi F Gazdar for the cell line.

Conflict of Interest Statement: None declared.

References

1. Carbone,M. *et al.* (2002) The pathogenesis of mesothelioma. *Semin. Oncol.*, **29**, 2–17.
2. Pass,H.I. *et al.* (2004) Malignant pleural mesothelioma. *Curr. Probl. Cancer*, **28**, 93–174.
3. Robinson,B.W. *et al.* (2005) Advances in malignant mesothelioma. *N. Engl. J. Med.*, **353**, 1591–1603.
4. Ramos-Nino,M.E. *et al.* (2006) Cellular and molecular parameters of mesothelioma. *J. Cell. Biochem.*, **98**, 723–734.
5. Vogelzang,N.J. *et al.* (2003) Phase III study of pemetrexed in combination with cisplatin versus cisplatin alone in patients with malignant pleural mesothelioma. *J. Clin. Oncol.*, **21**, 2636–2644.
6. van Meerbeeck,J.P. *et al.* (2005) Randomized phase III study of cisplatin with or without raltitrexed in patients with malignant pleural mesothelioma: an intergroup study of the European Organisation for Research and Treatment of Cancer Lung Cancer Group and the National Cancer Institute of Canada. *J. Clin. Oncol.*, **23**, 6881–6889.
7. Ascoli,V. *et al.* (2001) DNA copy number changes in familial malignant mesothelioma. *Cancer Genet. Cytogenet.*, **127**, 80–82.
8. Sugarbaker,D.J. *et al.* (2008) Transcriptome sequencing of malignant pleural mesothelioma tumors. *Proc. Natl Acad. Sci. USA*, **105**, 3521–3526.
9. Ladanyi,M. (2005) Implications of P16/CDKN2A deletion in pleural mesotheliomas. *Lung Cancer*, **49** (suppl. 1), S95–S98.
10. Musti,M. *et al.* (2006) Cytogenetic and molecular genetic changes in malignant mesothelioma. *Cancer Genet. Cytogenet.*, **170**, 9–15.
11. Pei,J. *et al.* (2006) High-resolution analysis of 9p loss in human cancer cells using single nucleotide polymorphism-based mapping arrays. *Cancer Genet. Cytogenet.*, **170**, 65–68.
12. Sekido,Y. *et al.* (1995) Neurofibromatosis type 2 (NF2) gene is somatically mutated in mesothelioma but not in lung cancer. *Cancer Res.*, **55**, 1227–1231.
13. Bianchi,A.B. *et al.* (1995) High frequency of inactivating mutations in the neurofibromatosis type 2 gene (NF2) in primary malignant mesotheliomas. *Proc. Natl Acad. Sci. USA*, **92**, 10854–10858.
14. Cheng,J.Q. *et al.* (1999) Frequent mutations of NF2 and allelic loss from chromosome band 22q12 in malignant mesothelioma: evidence for a two-hit mechanism of NF2 inactivation. *Genes Chromosomes Cancer*, **24**, 238–242.
15. Baser,M.E. (2006) The distribution of constitutional and somatic mutations in the neurofibromatosis 2 gene. *Hum. Mutat.*, **27**, 297–306.
16. Sun,C.X. *et al.* (2002) Protein 4.1 tumor suppressors: getting a FERM grip on growth regulation. *J. Cell Sci.*, **115**, 3991–4000.
17. McClatchey,A.I. *et al.* (2005) Membrane organization and tumorigenesis—the NF2 tumor suppressor, Merlin. *Genes Dev.*, **19**, 2265–2277.
18. Taniguchi,T. *et al.* (2007) Genomic profiling of malignant pleural mesothelioma with array-based comparative genomic hybridization shows frequent non-random chromosomal alteration regions including JUN amplification on 1p32. *Cancer Sci.*, **98**, 438–446.
19. Komuro,A. *et al.* (2003) WW domain-containing protein YAP associates with ErbB-4 and acts as a co-transcriptional activator for the carboxyl-terminal fragment of ErbB-4 that translocates to the nucleus. *J. Biol. Chem.*, **278**, 33334–33341.
20. Osada,H. *et al.* (2005) ASH1 gene is a specific therapeutic target for lung cancers with neuroendocrine features. *Cancer Res.*, **65**, 10680–10685.
21. Basu,S. *et al.* (2003) Akt phosphorylates the Yes-associated protein, YAP, to induce interaction with 14-3-3 and attenuation of p73-mediated apoptosis. *Mol. Cell*, **11**, 11–23.
22. Hayashita,Y. *et al.* (2005) A polycistronic microRNA cluster, miR-17-92, is overexpressed in human lung cancers and enhances cell proliferation. *Cancer Res.*, **65**, 9628–9632.
23. Heintz,N.H. *et al.* (1993) Persistent induction of c-fos and c-jun expression by asbestos. *Proc. Natl Acad. Sci. USA*, **90**, 3299–3303.
24. Mariani,O. *et al.* (2007) JUN oncogene amplification and overexpression block adipocytic differentiation in highly aggressive sarcomas. *Cancer Cell*, **11**, 361–374.
25. Zender,L. *et al.* (2006) Identification and validation of oncogenes in liver cancer using an integrative oncogenomic approach. *Cell*, **125**, 1253–1267.
26. Overholtzer,M. *et al.* (2006) Transforming properties of YAP, a candidate oncogene on the chromosome 11q22 amplicon. *Proc. Natl Acad. Sci. USA*, **103**, 12405–12410.
27. Huang,J. *et al.* (2005) The Hippo signaling pathway coordinately regulates cell proliferation and apoptosis by inactivating Yorkie, the *Drosophila* Homolog of YAP. *Cell*, **122**, 421–434.
28. Mohler,P.J. *et al.* (1999) Yes-associated protein 65 localizes p62(c-Yes) to the apical compartment of airway epithelia by association with EBP50. *J. Cell Biol.*, **147**, 879–890.
29. Murthy,A. *et al.* (1998) NHE-RF, a regulatory cofactor for Na(+)-H+ exchange, is a common interactor for merlin and ERM (MERM) proteins. *J. Biol. Chem.*, **273**, 1273–1276.
30. Bissig,H. *et al.* (1999) Evaluation of the clonal relationship between primary and metastatic renal cell carcinoma by comparative genomic hybridization. *Am. J. Pathol.*, **155**, 267–274.
31. Imoto,I. *et al.* (2001) Identification of cIAP1 as a candidate target gene within an amplicon at 11q22 in esophageal squamous cell carcinomas. *Cancer Res.*, **61**, 6629–6634.

32. Dai,Z. *et al.* (2003) A comprehensive search for DNA amplification in lung cancer identifies inhibitors of apoptosis cIAP1 and cIAP2 as candidate oncogenes. *Hum. Mol. Genet.*, **12**, 791–801.
33. Baldwin,C. *et al.* (2005) Multiple microalterations detected at high frequency in oral cancer. *Cancer Res.*, **65**, 7561–7567.
34. Zanazzi,C. *et al.* (2007) Gene expression profiling and gene copy-number changes in malignant mesothelioma cell lines. *Genes Chromosomes Cancer*, **46**, 895–908.
35. Hamaratoglu,F. *et al.* (2006) The tumour-suppressor genes NF2/Merlin and Expanded act through Hippo signalling to regulate cell proliferation and apoptosis. *Nat. Cell Biol.*, **8**, 27–36.
36. Pan,D. (2007) Hippo signaling in organ size control. *Genes Dev.*, **21**, 886–897.
37. Zhao,B. *et al.* (2007) Inactivation of YAP oncoprotein by the Hippo pathway is involved in cell contact inhibition and tissue growth control. *Genes Dev.*, **21**, 2747–2761.
38. Yagi,R. *et al.* (1999) A WW domain-containing yes-associated protein (YAP) is a novel transcriptional co-activator. *EMBO J.*, **18**, 2551–2562.
39. Vitolo,M.I. *et al.* (2007) The RUNX2 transcription factor cooperates with the YES-associated protein, YAP65, to promote cell transformation. *Cancer Biol. Ther.*, **6**, 856–863.
40. Aqeilan,R.I. *et al.* (2005) WW domain-containing proteins, WWOX and YAP, compete for interaction with ErbB-4 and modulate its transcriptional function. *Cancer Res.*, **65**, 6764–6772.
41. Vassilev,A. *et al.* (2001) TEAD/TEF transcription factors utilize the activation domain of YAP65, a Src/Yes-associated protein localized in the cytoplasm. *Genes Dev.*, **15**, 1229–1241.
42. Strano,S. *et al.* (2001) Physical interaction with Yes-associated protein enhances p73 transcriptional activity. *J. Biol. Chem.*, **276**, 15164–15173.
43. Strano,S. *et al.* (2005) The transcriptional coactivator Yes-associated protein drives p73 gene-target specificity in response to DNA damage. *Mol. Cell*, **18**, 447–459.
44. Matallanas,D. *et al.* (2007) RASSF1A elicits apoptosis through an MST2 pathway directing proapoptotic transcription by the p73 tumor suppressor protein. *Mol. Cell*, **27**, 962–975.
45. Xiao,G.H. *et al.* (2005) The NF2 tumor suppressor gene product, merlin, inhibits cell proliferation and cell cycle progression by repressing cyclin D1 expression. *Mol. Cell. Biol.*, **25**, 2384–2394.
46. Poulikakos,P.I. *et al.* (2006) Re-expression of the tumor suppressor NF2/merlin inhibits invasiveness in mesothelioma cells and negatively regulates FAK. *Oncogene*, **25**, 5960–5968.
47. Lee,H. *et al.* (2007) Identification and characterization of putative tumor suppressor NGB, a GTP-binding protein that interacts with the neurofibromatosis 2 protein. *Mol. Cell. Biol.*, **27**, 2103–2119.
48. Fleury-Feith,J. *et al.* (2003) Hemizygosity of Nf2 is associated with increased susceptibility to asbestos-induced peritoneal tumours. *Oncogene*, **22**, 3799–3805.
49. Altomare,D.A. *et al.* (2005) A mouse model recapitulating molecular features of human mesothelioma. *Cancer Res.*, **65**, 8090–8095.
50. Jongsma,J. *et al.* (2008) A conditional mouse model for malignant mesothelioma. *Cancer Cell*, **13**, 261–271.

Received April 9, 2008; revised August 10, 2008; accepted August 20, 2008

Clinical Relevance of Sputum Cytology and Chest X-Ray in Patients with Suspected Lung Tumors

Mitsuhiro Sumitani, Nobuhide Takifuji, Shigeki Nanjyo, Yumiko Imahashi, Hidemi Kiyota, Koji Takeda, Ryoji Yamamoto and Hirohito Tada

INTERNAL MEDICINE

Reprinted from Internal Medicine
Vol. 47, Pages 1199-1205
July 2008